1-1-1981

Areal Distribution, Thickness, Mass, Volume, and Grain Size of Air-Fall Ash from the Six Major Eruptions of 1980

Andrei M. Sarna-Wojcicki

Susan Shipley

Richard B. Waitt Jr.

Daniel Dzurisin

Spencer H. Wood
Boise State University

THE 1980 ERUPTIONS OF MOUNT ST. HELENS, WASHINGTON

AREAL DISTRIBUTION, THICKNESS, MASS, VOLUME, AND GRAIN SIZE OF AIR-FALL ASH FROM THE SIX MAJOR ERUPTIONS OF 1980

By ANDREI M. SARNA-WOJCICKI, SUSAN SHIPLEY, RICHARD B. WAITT, JR., DANIEL DZURISIN, *and* SPENCER H. WOOD[1]

ABSTRACT

The airborne-ash plume front from the Mount St. Helens eruption of May 18 advanced rapidly to the northeast at an average velocity of about 250 km/hr during the first 13 min after eruption. It then traveled to the east-northeast within a high-velocity wind layer at altitudes of 10–13 km at an average velocity of about 100 km/hr over the first 1,000 km. Beyond about 60 km, the thickest ash fall was east of the volcano in Washington, northern Idaho, and western Montana. A distal thickness maximum near Ritzville, Wash., is due to a combination of factors: (1) crude sorting within the vertical eruptive column, (2) eruption of finer ash above the high-velocity wind layer at altitudes of 10–13 km, and (3) settling of ash through and below that layer. Isopach maps for the May 25, June 12, August 7, and October 16–18 eruptions show distal thickness maximums similar to that of May 18.

A four-unit tephra stratigraphy formed by the May 18 air fall within proximal areas east of the volcano changes to three units, two units, and one unit at progressively greater distances downwind. Much of the deposit beyond 200 km from the volcano has two units. A lower thin dark lithic ash is inferred to represent products that disintegrated from the volcano's summit in the initial part of the eruption and early juvenile pumice and glass. An upper, thicker, light-gray ash rich in pumice and volcanic-glass shards represents the later voluminous eruption of juvenile magma. The axis of the dark-ash lobe in eastern Washington and northern Idaho is south of the axis of the light-gray ash lobe because the high-velocity wind layer shifted northward during the eruption. The areal distribution of ash on the ground is offset to the north relative to the mapped position of the airborne-ash plume, because the winds below the high-velocity wind layer were more northward.

Except for the distal thickness near Ritzville, Wash., mass per area, thickness, and bulk density of the May 18 ash decrease downwind, because larger grains and heavier lithic and crystal grains settled out closer to the volcano than did the lighter pumice and glass shards. A minimum volume of 1.1 km^3 of uncompacted tephra is estimated for the May 18 eruption; this volume is equivalent to about 0.20–0.25 km^3 of solid rock, assuming an average density of between 2.0 and 2.6 g/cm^3 for magma and summit rocks. The estimated total mass from the May 18 eruption is 4.9×10^{14} g, and the average uncompacted bulk density for downwind ash is 0.45 g/cm^3. Masses and volumes for the May 25 and June 12 eruptions are an order of magnitude smaller than those of May 18, but average bulk densities are higher (about 1.00 and 1.25), owing to compaction by rain that fell during or shortly after the two eruptions. Volume and mass of the July 22 eruption are two orders of magnitude smaller than those of May 18, and those of the August 7 and October 16–18 eruptions are three orders of magnitude smaller. The eruption of May 18, however, is smaller than five of the last major eruptions of Mount St. Helens in terms of volume of air-fall tephra produced, but probably is intermediate if the directed-blast deposit is included with the air-fall tephra.

INTRODUCTION

The eruption of Mount St. Helens on May 18, 1980, and the succeeding major eruptions present an excellent opportunity to study dispersal patterns and

[1]Boise State University, Boise, Idaho, 83725.

depositional characteristics of windborne ash. Many large historic volcanic eruptions have occurred on islands or peninsulas adjacent to oceanic areas or in areas of difficult access. Where volcanoes have been accessible to direct observation, most downwind ash plumes have been carried across ocean areas, and the areal extent, thickness, grain size, and mass of ash could not be fully documented. Specific eruptions in point are Tamboro (1815), Krakatoa (1883), Katmai (1912), Hekla (1974), and Bezymianny (1956). Quizapú volcano (1932), however, is a notable exception. The May 18 eruption of Mount St. Helens occurred on land, and the ash plume was carried eastward across accessible areas where observations could be readily made on the ground. In addition, owing to technological developments within recent years, satellite imagery was available to track the areal extent and progress of an airborne-ash plume.

We mapped the areal distribution of an airborne-ash plume, charted its downwind progress, and compared its airborne distribution with the distribution of the ash lobe on the ground. Several geologists sampled across the ash lobe shortly after the ash had fallen; therefore, various characteristics were documented before the ash was disrupted by wind or rain. Because each geologist conducted a traverse completely across the fallen-ash lobe, using the same methods and observational criteria, a coherent, compatible data base was provided.

ACKNOWLEDGMENTS

This report is the result of a large cooperative effort by many individuals who contributed observations, samples, and other help and information. We are particularly grateful to T. E. Bateridge, J. O. Davis, W. H. Hays, M. P. Doukas, James Beget, Evelyn Newman, Robert Mark, Carol Price, Daniel May, Albert Eggars, Carolyn Driedger, Harry Glicken, Michael Ryan, M. W. Brugman, David Sawyer, and C. C. Helicker for conducting sampling traverses across tephra lobes.

We are also grateful to R. P. Hoblitt, P. L. Weis, Barry Voight, Thor Kiilsgaard, C. F. Kienle, Jr., Sandra Embrey, Edwin Olson, Gregory Hahn, J. A. Barker, Brian Atwater, Kenneth Fox, F. K. Miller, J. W. Nichols, Mrs. David Mahre, W. P. Nash, Bruce Cochran, C. R. Knowles, Lynn Disbrow, Lester Zeiheu, Glen Izett, Carl Rice, Edwin Danielson, Robert Courson, Robert Quinn, Michael Folsom, Daisuke Shimozuru, E. F. Hubbard, Steve Frenzel, Marv Fretwell, David Frank, D. P. Dethier, Norman Banks, R. R. Hooper, T. A. Cahill, R. E. Wilcox, James Bailey, John Strong, and D. B. Mitchell for providing samples, observational data, or other information.

We are grateful to Gail McCoy, who helped to compile thickness data and helped with grain-size analyses, and to Graig McHendrie, who helped with computer processing of grain-size data.

VERTICAL GROWTH AND DOWNWIND PROGRESS OF THE ASH PLUME FROM THE MAY 18 ERUPTION

A few minutes after the start of the eruption at 0832 PDT (Pacific Daylight time) on May 18, a vertical column of hot, ash-charged gas shot vertically from the volcano and grew rapidly to altitudes of 23 km or more. According to an airborne eyewitness, the vertical plume rose to an altitude of 7.6 km at 0838, to 10.7 km at 0840, and to about 18 km at 0842 (Rosenbaum and Waitt, this volume). The column expanded rapidly into a mushroom shape 10 min after the start of the eruption. By 0845, the time of the first satellite images after the start of the eruption, the ash plume had expanded to an ovoid lens about 80 km long in an east-west direction, 45 km wide in the north-south direction, and about 9–14 km in thickness (figs. 331, 332). At 0845 the top of the ash plume had risen to 23 km, and by 0900, to perhaps as much as 27 km (Carl Rice, oral commun., 1980). The average vertical rate of ascent of the column between 0838 and 0842 is 44 m/s, or about 160 km/hr (fig. 333). By 1012 the column had subsided to an altitude of about 13 km, but the eruption continued into the late afternoon.

The prevailing westerly wind swept the ash plume east-northeast. From a sequence of NOAA satellite photographs taken from stationary orbit at half-hour intervals between 0845 and 1816 on May 18 (fig. 332), we compiled an isochron map of the airborne-ash plume front. By 0945 the widening plume front passed over Yakima, Wash., 135 km downwind, and by about 1200, over Spokane, Wash., and Moscow, Idaho, about 400 km east of Mount St. Helens. By

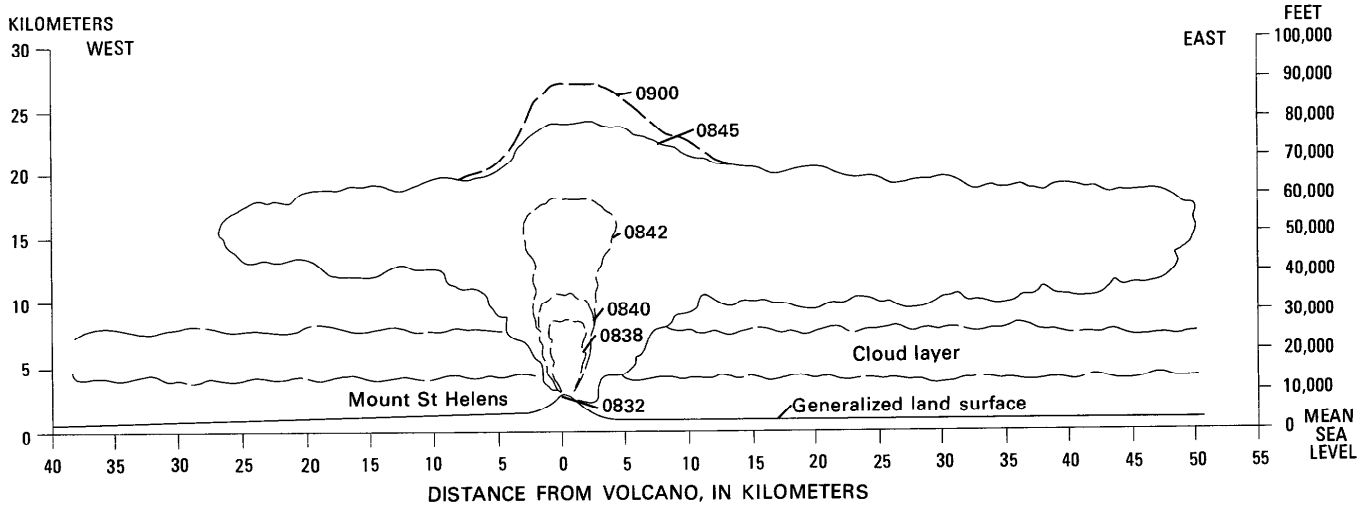

Figure 331.—Diagrammatic east-west profile showing early vertical growth and lateral expansion of plume from the May 18 eruption. Altitudes between 0838 and 0842 are from Rosenbaum and Waitt (this volume) and those between 0845 and 0900 are from Carl Rice (oral commun., 1980). Horizontal extent for 0845 is from NOAA satellite photograph taken at 0845 PDT, sector KB7.

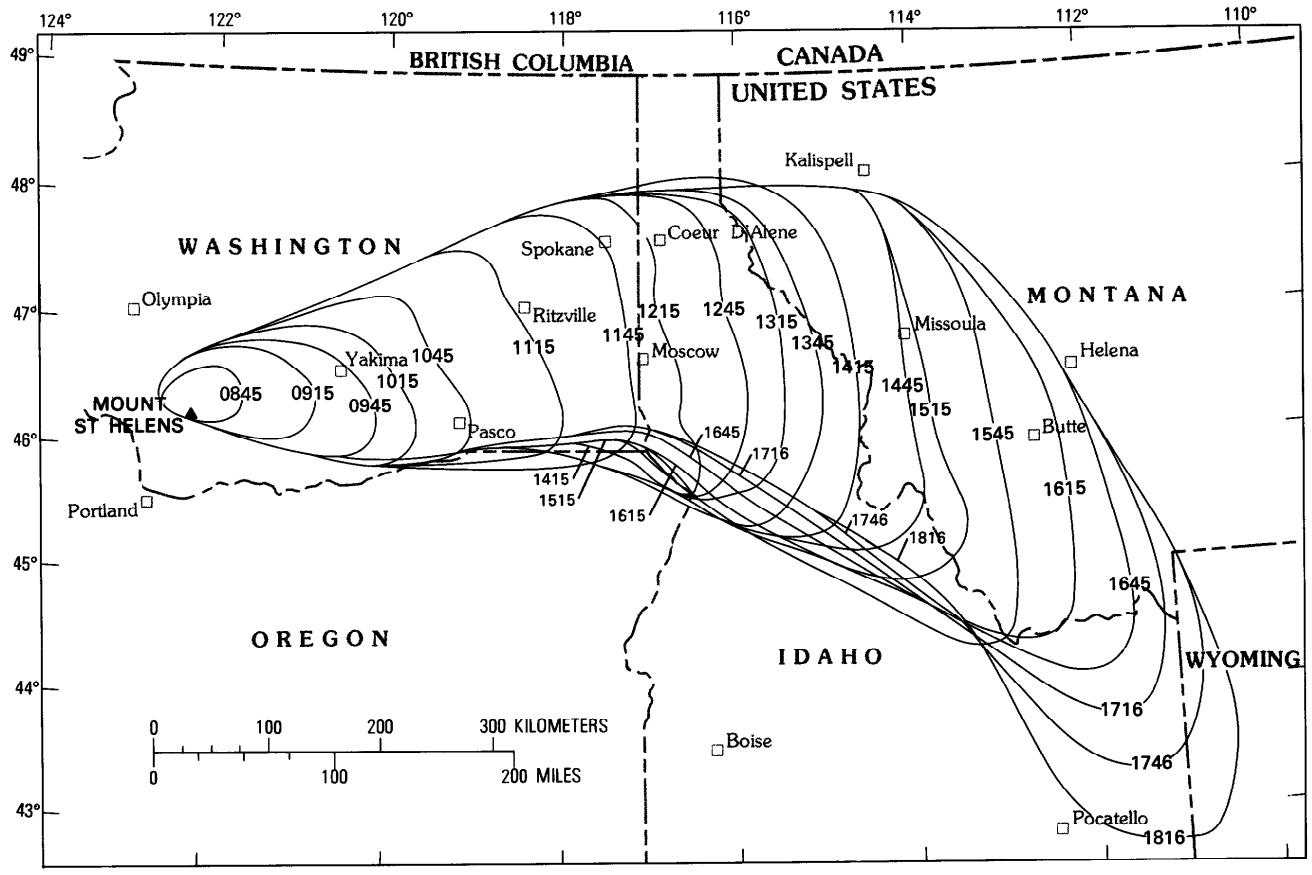

Figure 332.—Isochron map showing maximum downwind extent of ash from airborne-ash plume erupted from Mount St. Helens on May 18 and carried by fastest moving wind layer, as observed on satellite photographs. Map is compiled from NOAA satellite photographs (sectors KB7 and SA40) taken at half-hour intervals between 0845 and 1816 PDT. Plot of plume position relative to ground was visually corrected for zenith angle. Probable error in position of plume boundaries is ±10 km in the north-south direction, and ±5 km in the east-west direction.

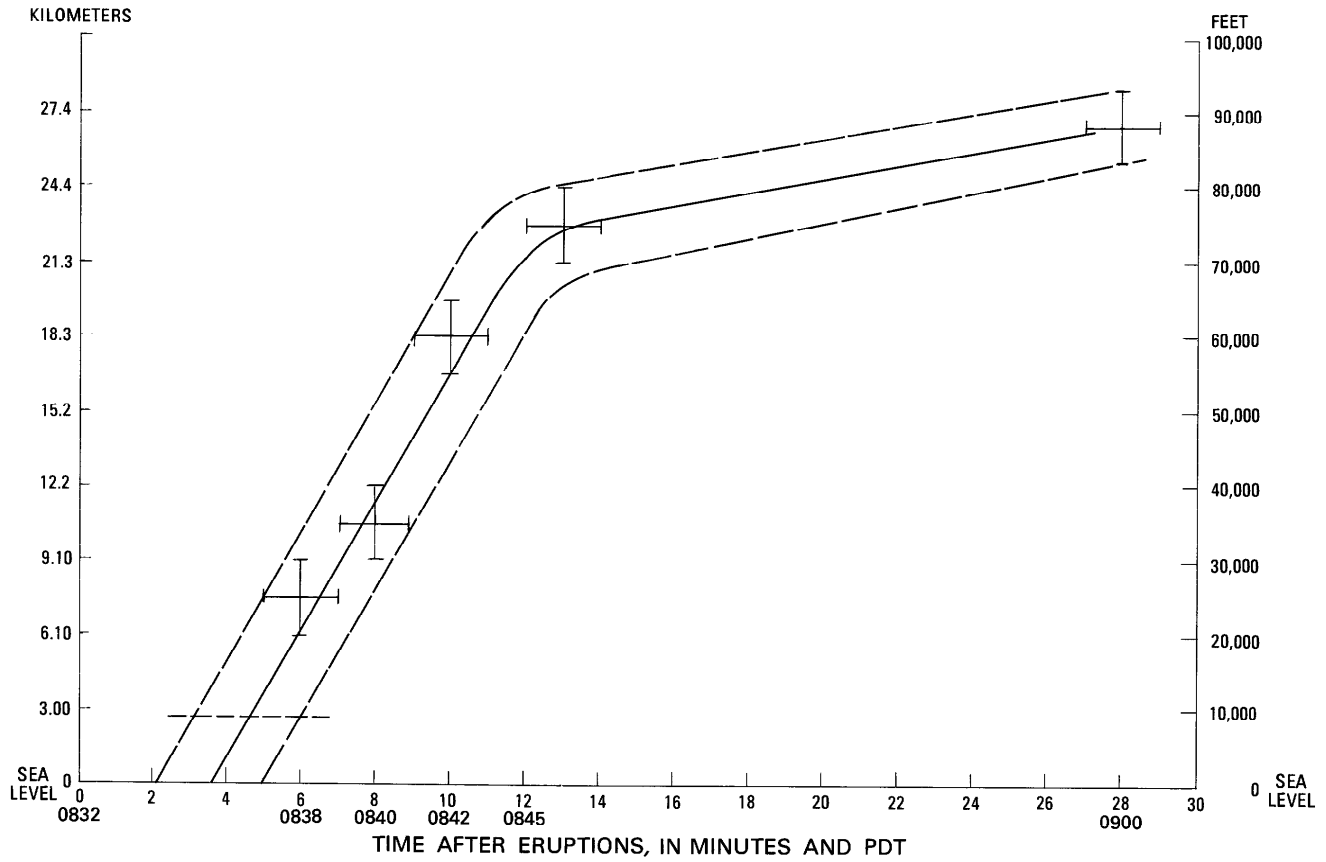

Figure 333.—Rate of ascent of vertical plume from eruption of May 18. Lower three data points are from eyewitness reports (Rosenbaum and Waitt, this volume). Upper two data points are from satellite observation (Carl Rice, oral commun., 1980). Bars indicate possible errors in time and altitude.

about 1500 the plume front had passed over Missoula, Mont., where changing wind directions swung the front to the southeast. By about 1800, the plume front had passed into northwestern Wyoming. After nightfall on May 18, the plume could not be monitored with visible-spectrum photographs, and infrared imagery was insufficient to define plume boundaries. By the morning of May 19, the ash plume had passed into the midcontinent, where its margins became so diffuse and mixed with clouds that its boundaries could not be accurately detected. The densest part of the ash plume, however, was tracked across the plains to the East-Central United States, where it swung northeast over New England, Maritime Provinces of Canada, and out over the North Atlantic Ocean. Traveling eastward, the ash plume returned over the West Coast of North America in early June after circling the globe (Danielson, 1980). Although high-velocity winds at altitudes of 10–13 km carried the main body of ash eastward, higher stratospheric winds carrying some fine ash looped over the Northwestern United States, then veered westward and carried the finest ash over the North Pacific Ocean (Danielson, 1980).

The heaviest ash fall from the plume east of Mount St. Helens was observed in Washington, northern Idaho, and western Montana; lighter ash fall was reported in Wyoming, western South Dakota, western Nebraska, Colorado, and northern New Mexico. Light dustings were sporadically reported farther east and northeast. The finest ash, which remains suspended in the atmosphere, has circled the Earth many times; on the basis of the effects from historic eruptions such as Krakatoa in 1883 (G. J. Symons, 1888), it is likely to remain suspended in the atmosphere for years.

We derived a traveltime curve (fig. 334) for the front part of the plume from figure 332 by plotting the time the plume traveled since the start of the eruption against the maximum horizontal distance it traveled between each satellite photograph. Plume-front velocities calculated from satellite imagery give

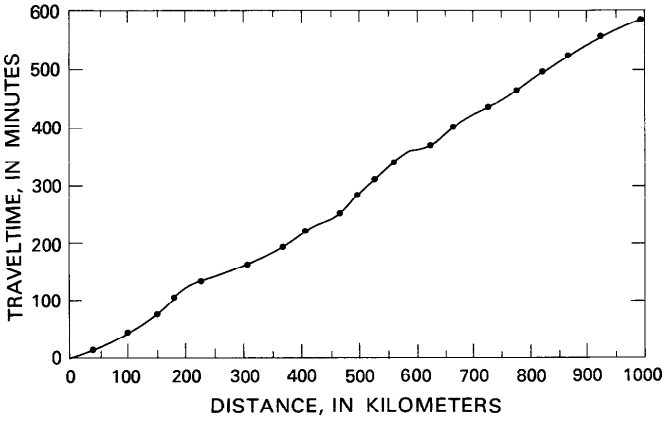

Figure 334.—Traveltime versus distance from the volcano for airborne-ash plume from the May 18 eruption. Traveltimes were calculated from a trajectory at approximately maximum distances from the volcano, as determined from NOAA satellite photographs (fig. 332).

estimates of the horizontal component of velocity only. An average horizontal component of velocity of the tephra plume front for the first 13 min is about 250 km/hr. The average azimuth of maximum velocity 13 min from the start of the eruption is about 040° from the volcano. This azimuth is intermediate between the predominantly northward direction of the initial directed blast and the 058° azimuth of the axis of the air-fall lobe that was determined from subsequent thickness measurements on the ground. This relation suggests that the initial directed-blast cloud was rapidly swept toward a more easterly direction by the prevailing wind. Because the 250-km/hr velocity represents an average over the first 13 min, and because the plume-front velocity decreased after the first 13 min, velocities of the expanding ash cloud in the first few minutes of the eruption must have been much greater. Average velocities of the ash-plume front over the first 13 min, as calculated from satellite photographs, were only about 220 km/hr in the direction of the prevailing wind, about 185 km/hr northward, about 150 km/hr northwestward, and zero to the south and southwest. The velocity of the plume front averaged about 100 km/hr as it traveled east-northeast over the first 1,000 km. Fine ash erupted above the level of high-velocity winds (above 13 km altitude) was carried at lower velocities along different trajectories (Danielson, 1980).

We do not have accurate altitude control for the ash-plume front as it traveled east-northeast. The base of the leading edge of the plume was reported to be at about 11.9–12.2 km, which corresponds to the high-velocity air layer along much of its observed route in the Western States, but diffuse parts of the downwind plume were observed to altitudes of about 21.3 km (Edwin Danielson, NASA-Ames, oral commun., 1980). Typical wind profiles at Spokane, Wash., for the period 1600 on May 17 to 0400 on May 19 (fig. 335), show velocity maximums at altitudes of 10.7–12.2 km. Low-level winds were more northward than were the high-level winds (fig. 335), which offset the ash lobe on the ground to the north relative to the position of the airborne cloud.

AREAL EXTENT AND THICKNESS OF ASH FROM THE MAY 18 ERUPTION

During traverses across the ash lobe, uncompacted thickness of ash was measured, and samples were collected from measured areas to determine the mass per area. Samples were collected from surfaces that were generally free of ground litter or dust prior to the eruption—from vehicles, shed roofs, and other artificial surfaces away from heavily traveled roads. The initial uncompacted thicknesses were measured before the first rain on May 21. Because most of the traverse through Ritzville, Wash., was made on May 21 and 22 after rain had begun, thickness values there were lower than those made before rain had started. We have adjusted the thickness values along this traverse by using associated mass-per-area values, and by comparing these values to mass-per-area values and associated uncompacted thicknesses along adjacent traverses that were measured before rain had started. Adjusted initial thicknesses for the Ritzville, Wash., traverse are on the average twice those measured after the rainfall.

The "saddle" near Vantage, Wash., and the distal thickness maximum near Ritzville, Wash. (figs. 336, 337), are unusual. This type of distribution has been documented only once—for the 1932 eruption of Quizapu (Larsson, 1937). Isopach maps for eruptions of May 25, June 12, August 7, and October 16–18 show similar distal thickness; thus, such features may be fairly common. Because these distal thickness highs were formed on fair days as well as rainy, they cannot be attributed to scavenging of ash by rain, a mechanism suggested for anomalous distributions of downwind thickness by Wilcox (1959).

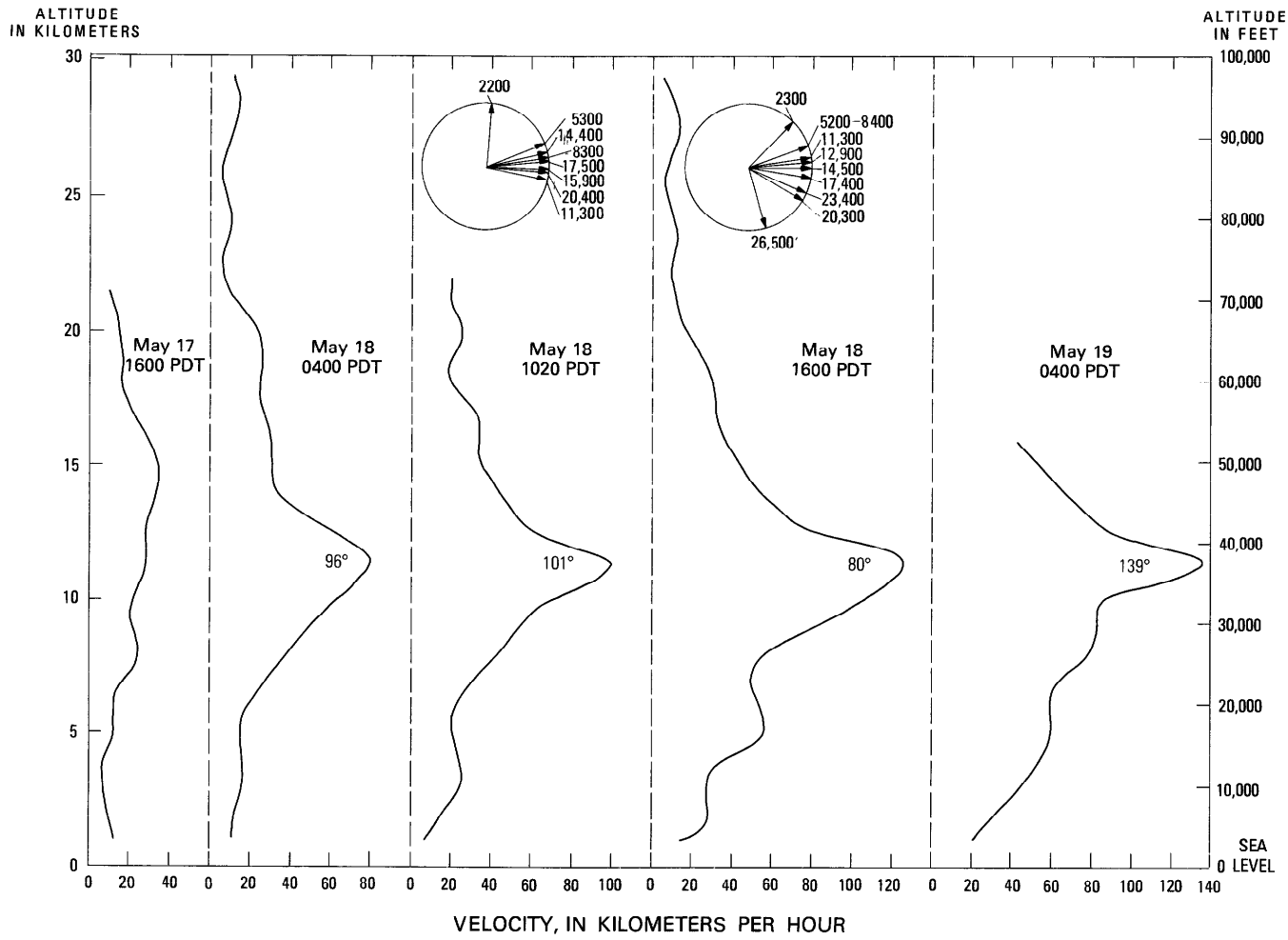

Figure 335.—Average wind-speed profiles from measurements at Spokane, Wash., between May 17 and May 19, by the U.S. National Meteorological Service. Data were averaged for intervals of about 1,500 m (5,000 ft). Average direction toward which the wind was blowing is shown in degrees, adjacent to the high-velocity wind layer. Circular wind diagrams show average directions toward which the wind was blowing at different altitudes, at 1020 and 1600 PDT on May 18 at Spokane, Wash.

We do not understand how the distal thickness maximum near Ritzville, Wash., formed. Major factors controlling downwind distribution of tephra in an eruption such as that of May 18 are the height of the vertical eruptive column, the size range and distribution of ejecta, the velocities and directions of wind at different altitudes above the volcano and downwind, and the manner in which these factors vary with time. The vertical eruption column, which extended above the high-velocity wind layer for much of the day, probably acted as a crude sorting mechanism. J. G. Moore (written commum., 1980) suggested that the distal thickness maximum near Ritzville, Wash., formed from fallout of ash that was erupted above the high-velocity wind layer; the thickness low near Yakima, Wash., formed from ash injected into the high-velocity layer; and the primary areas of maximum thickness near the volcano formed from ejecta erupted below the high-velocity layer.

Along the easternmost traverse through Missoula, Mont., ash was too thin in most places to measure directly. Thicknesses for this traverse were estimated by comparing an average of three uncompacted thicknesses in Missoula, where the ash was thick enough to measure, with the average of associated masses per area. Thicknesses at other sampled sites in

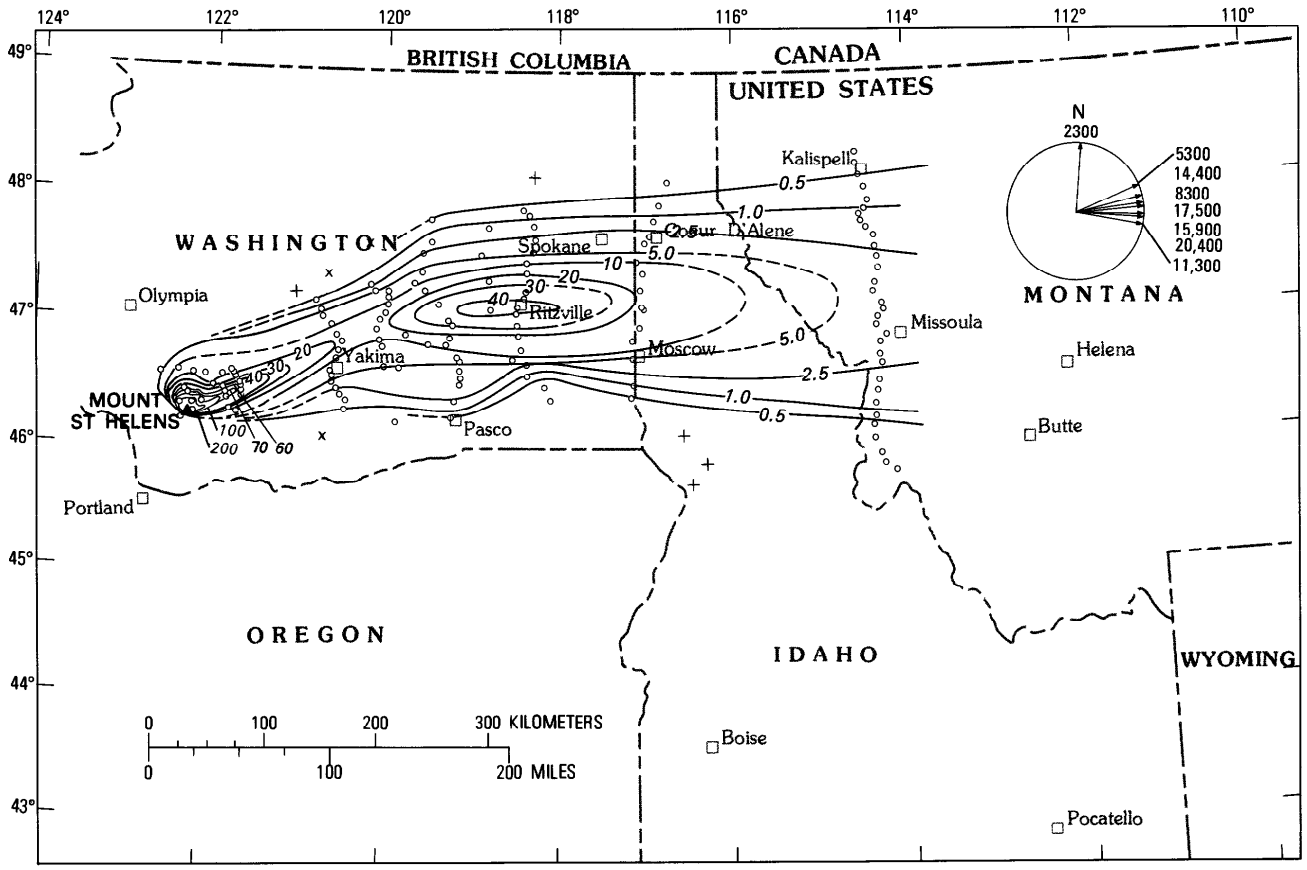

Figure 336.—Isopach map of air-fall ejecta on May 18. Lines represent uncompacted thickness, in millimeters. +, light dusting of ash; x, no ash observed; circles, observation sites. Circular diagram shows average directions toward which wind was blowing, for different altitudes, at 1020 PDT on May 18, at Spokane, Wash. Data from U.S. National Meteorological Service. Thicknesses along north-south traverse through Ritzville and at four observation sites about 30–50 km to the west have been adjusted for postdepositional compaction due to rain. Ash along north-south traverse through Missoula was too thin to measure directly, and thicknesses have been calculated from mass per area, using thickness and associated mass per unit area measured near Missoula. Data on north-south traverse through Ritzville and four sites 30–50 km to the west from J. O. Davis. Data on north-south traverse through Missoula from Thomas Bateridge. Data in vicinity of Spokane from Paul Weis.

this traverse were calculated by applying this ratio to the known mass per area at each site.

Sampling traverses were not made east of western Montana, though spot thicknesses were reported farther east and southeast in Montana and Wyoming. Only a light "dusting" of ash fell farther downwind than Wyoming. Some reports of thicknesses within our map area by other observers were much higher than those stated in this report; for example, maximum thicknesses more than two times those reported in this study were observed by USGS personnel about 54 km north of Moscow, Idaho, near the axis of the May 18 ash plume (fig. 336) (Ernest F. Hubbard, oral commun., 1980). Hooper and others (1980) reported ash 1.25 cm thick in Moscow, Idaho, whereas we measured 0.4 cm on May 20 and 21. There are several possible reasons for these discrepancies: First, where observations were made prior to ours, initial uncompacted thicknesses may have been greater owing to greater initial cohesion between ash particles. Second, some observers may have reported maximum rather than average thicknesses. Thicknesses shown in figure 336 are the same as or lower than those reported by others. Our measurements are internally consistent and agree with isomass data that are based on independent measurements. Because some compaction

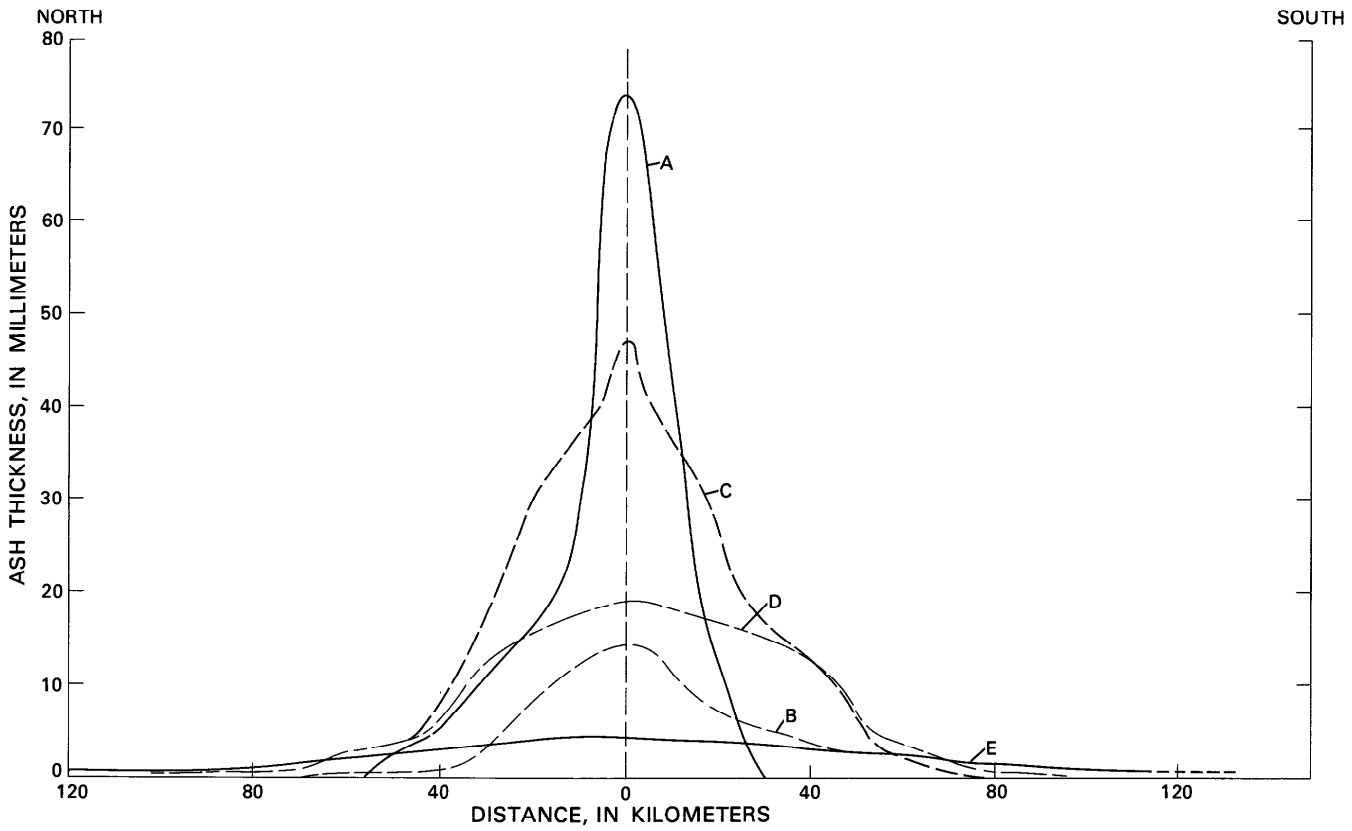

Figure 337.—Profiles across tephra lobe, normal to plume axis. Profiles are centered on axis at the following distances downwind from the eruption: A, 40 km; B, 170 km; C, 315 km (secondary thickness maximum near Ritzville); D, 415 km; E, 630 km.

undoubtedly occurred before some ash was measured, our estimate of initial bulk volume is a minimum. Initial uncompacted thickness is an ephemeral parameter that is not easily measured; consequently, it is not as reliable as isomass or compacted thickness.

MASS AND BULK DENSITY OF FALLEN ASH FROM THE MAY 18 ERUPTION

Compaction due to loading, wind, rain, or time will not affect measurements of mass, because mass per area is unchanged by compaction. Samples collected from measured areas were weighed, and mass per unit area was contoured (fig. 338). The shape of the isomass map is generally the same as that of the isopach map (fig. 336).

We estimated uncompacted bulk densities for individual observation sites by dividing the uncompacted thickness into the the mass per unit area. Thickness, mass, bulk density, and mean grain size generally decrease with distance from the volcano (figs. 339, 342). The decrease in bulk density reflects the depletion of crystal and lithic grains and the relative enrichment of the lighter pumice and glass shards downwind. This effect has been documented in other studies (Larsson, 1937). Packing of grains also plays a large if not dominant role in the decrease of bulk density downwind. Compaction by rain alone commonly effects a twofold increase in bulk density, indicating that newly fallen ash was very loosely packed. The angular and irregular glass and pumice shards that compose a progressively greater portion of low-density downwind ash are more loosely packed than are the denser, more equant crystal and lithic grains. The average bulk density calculated for Missoula, Mont., is very low (0.11 g/cm^3), although the data on uncompacted thickness there are sparse, and the error in measuring the very thin layer of ash is significant.

STRATIGRAPHY, GRAIN SIZE, AND AREAL DISTRIBUTION OF DOWNWIND ASH

Proximal stratigraphy of the May 18 air-fall deposits northeast of the volcano, along the axis of the downwind lobe, consists of four units referred to as units A through D (Waitt and Dzurisin, this volume). This stratigraphy changes progressively with distance downwind. Unit D can be traced only locally in proximal areas, and pinches out some distance west of Yakima, Wash., 135 km east-northeast of Mount St. Helens (fig. 339, *A*). The three layers observed 130 km downwind along the lobe axis north of Yakima are a basal, 1-mm-thick, gray silt-size ash (unit 1); an overlying, 1-mm-thick, "salt-and-pepper"-colored fine sand-size ash composed of lithic and crystal fragments and fine pumice shards (unit 2); and an uppermost, 17-mm-thick, fine sand- to silt-size light-gray to tan ash composed of pumice and glass shards, crystals, and minor lithic fragments (unit 3) (fig. 339). Unit 1 is the distal equivalent of proximal layer A3. Unit 2 is the distal equivalent of layer B1, a coarse "salt-and-pepper"-colored layer that contains abundant angular lithic fragments, small pumice lapilli, and crystals (Waitt and Dzurisin, this volume). Unit 3 is most probably a distal facies of layers B2 and B4, the thickest proximal layers that contain most of the coarse pumice (fig. 339). Unit 3 may also contain late-settling, fine low-density particles from the other proximal units A through D.

About 200–250 km downwind from Mount St. Helens along the lobe axis, unit 2 pinches out or merges with the basal unit. From Moses Lake, some

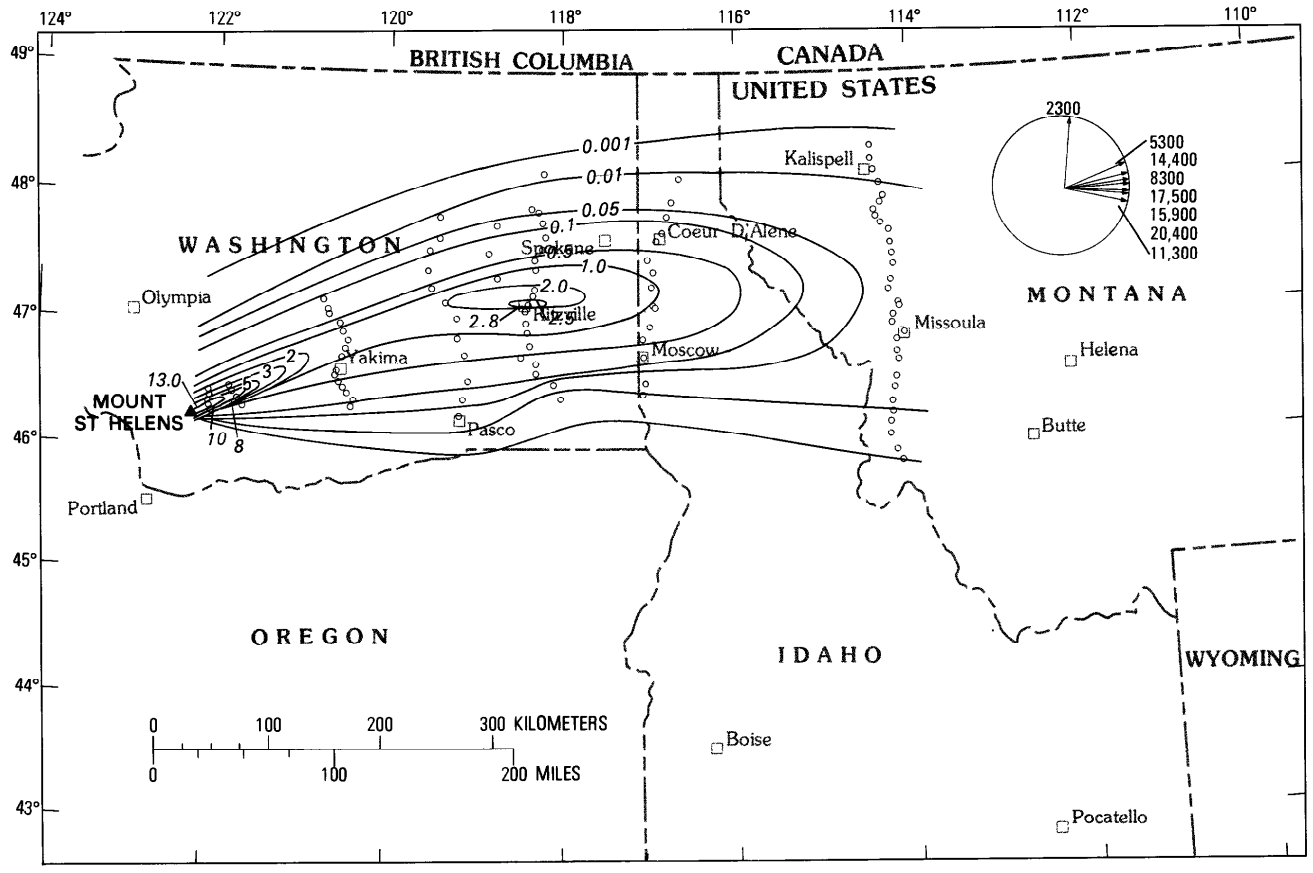

Figure 338.—Isomass map of ash erupted from Mount St. Helens on May 18. Lines represent mass of ash per area, in g/cm². Open circles represent observation stations. Circular diagram shows average directions toward which wind was blowing for different altitudes at 1020 PDT on May 18, at Spokane, Wash. Data from U.S. National Meteorological Service. Samples of ash were collected from measured, essentially horizontal surfaces, oven dried at 60°C for 12 hr, and weighed. Data on north-south traverse through Ritzville, Wash., and three sites 40–50 km to the west, from J. O. Davis. Data on north-south traverse through Missoula, Mont., from Thomas Bateridge.

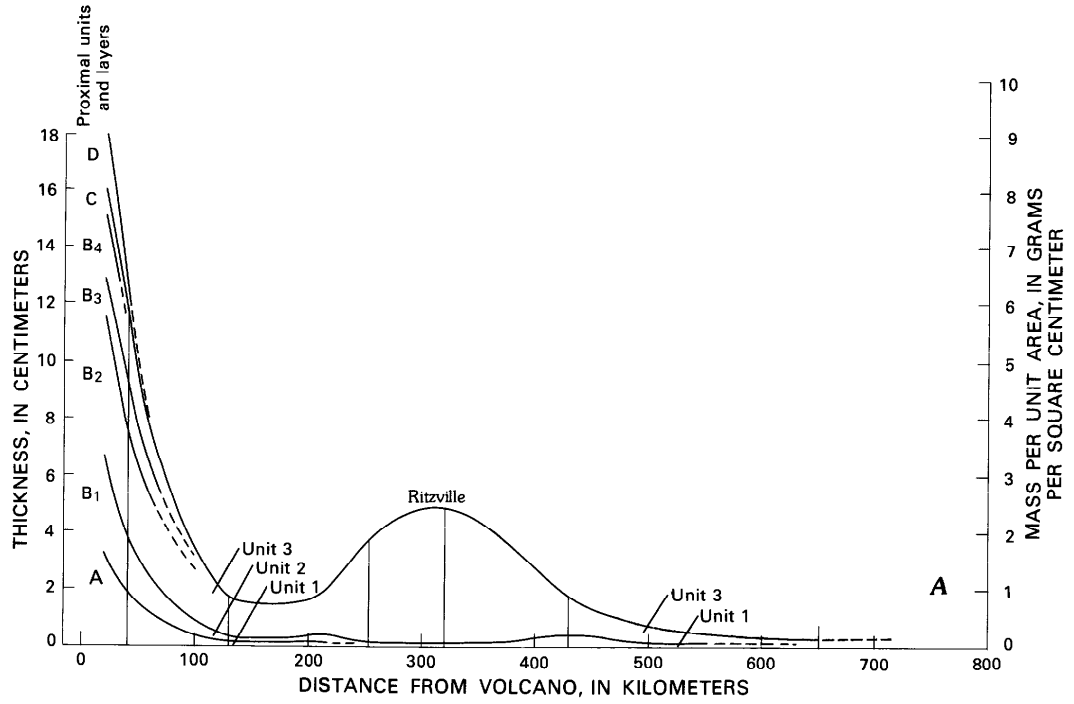
Proximal units and layers
D
C
B4
B3
B2
B1
A
Unit 3
Unit 2
Unit 1
Ritzville
Unit 3
Unit 1
A
THICKNESS, IN CENTIMETERS
MASS PER UNIT AREA, IN GRAMS PER SQUARE CENTIMETER
DISTANCE FROM VOLCANO, IN KILOMETERS

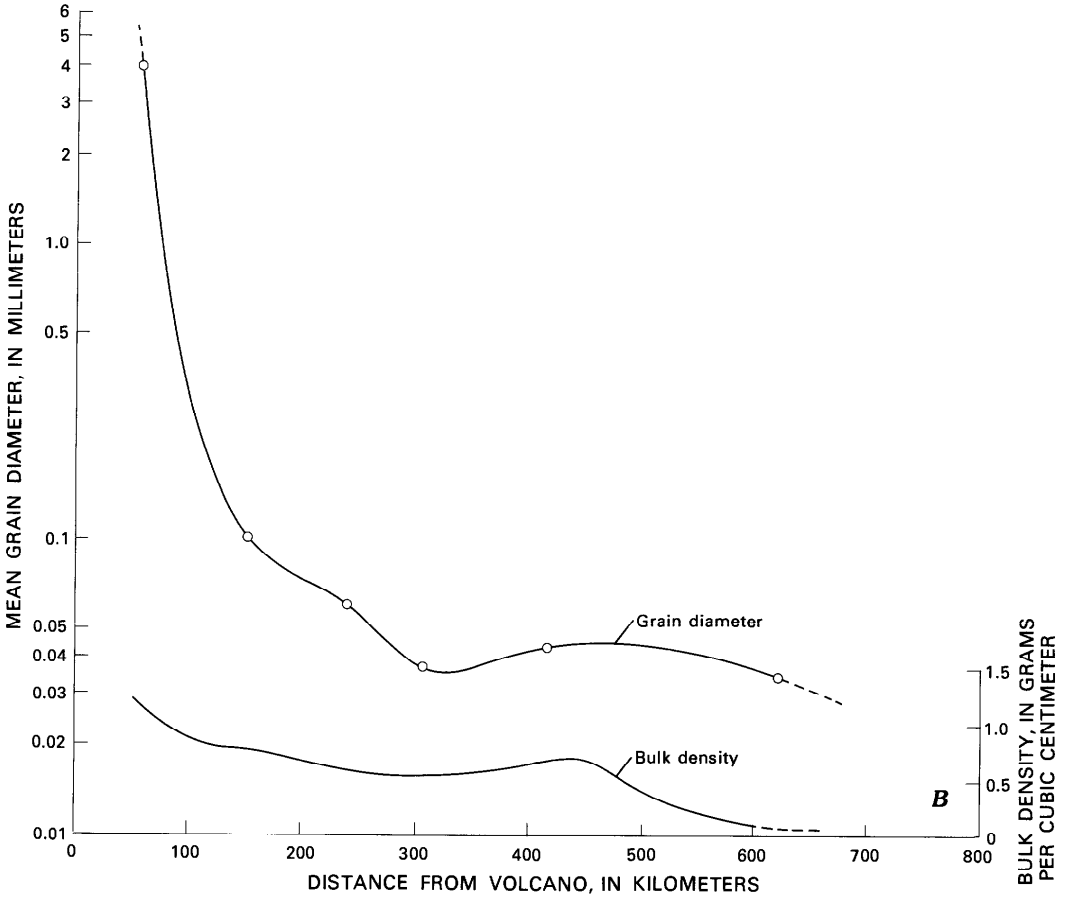
Grain diameter
Bulk density
B
MEAN GRAIN DIAMETER, IN MILLIMETERS
BULK DENSITY, IN GRAMS PER CUBIC CENTIMETER
DISTANCE FROM VOLCANO, IN KILOMETERS

250 km east of Mount St. Helens, to the western border of Idaho and to some undetermined distance beyond, the ash blanket consists of unit 1 and the thicker unit 3. Farther downwind, in western Montana, only a single light-gray layer was deposited. The basal unit may have pinched out or, more likely, the two layers have merged owing to mixing downwind.

The pronounced distal thickening of ash in the vicinity of Ritzville, Wash. (figs. 336, 339), is caused by the thickening of unit 3. Unit 1 also may have a distal thickness maximum between 400 and 500 km downwind along the lobe axis. This distal thickening of unit 1 may correlate with a high in bulk density and mean-grain diameter (fig. 339) at about the same distance.

The dark ash (unit 1) began to fall considerably before the light-colored ash (unit 3). At Spokane, Wash., the advancing ash cloud became visible about 1400, ash started falling about 1543, and daylight was noticeably obscured about 1545 (Paul Weis, written commun., 1980). Satellite photographs, however, indicate that the ash front passed over Spokane about 2 hr before the cloud was visible to the ground observer, except for a sun halo that appeared about 1215. This time difference suggests that the front of the ash cloud was diffuse. Similarly, dark ash fell at Pullman, Wash., from about 1400 until about 1615, when light-colored ash began to fall. The light-colored ash continued to fall until about 0200 on May 19 (Hooper and others, 1980). On the north-south traverse through Moscow, Idaho, the axis of the dark layer is about 40 km south of the axis of the light-colored layer (fig. 340); this difference suggests that deposition for each layer occurred under somewhat different wind conditions. At Missoula, Mont., ash fall began about 2000–2030, some $3\frac{1}{4}$ to $3\frac{3}{4}$ hr after the front passed, but near the north end of the traverse, ash fall began between 2100 and 2200, about $3\frac{1}{2}$ to $4\frac{1}{2}$ hr after the front passed. Both in eastern Washington and in western Montana, 2 hr or more elapsed between the passage of the ash-cloud front and the start of ash fall on the ground. The delay was greater on the north side of the plume than on the south side.

Figure 339.—Stratigraphy of May 18 air-fall deposits northeast of volcano, along axis of downwind lobe. A, Variation in stratigraphic units and thickness. B, Variation in mean grain size and uncompacted bulk density. Bulk-density profile was derived by dividing thickness curve into mass-per-area at corresponding distances from volcano. Contours dashed where uncertain.

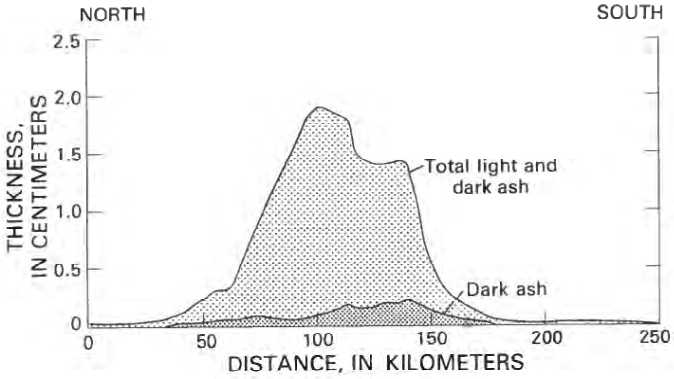

Figure 340.—Thickness of dark- and light-colored ash layers along the north-south traverse through Moscow, Idaho (see fig. 336 for location of traverse).

We compared the isochron map, which shows the approximate shape and areal dimensions of the airborne-ash plume, with the isomass map, which shows the minimum areal and mass distribution of the ash on the ground (fig. 341). The ash lobe on the ground is offset to the north relative to the position of the airborne plume. This northward shift of the air-fall lobe relative to the position of the airborne plume is a result of different wind directions with altitude. Much of the ash deposited from central Washington to western Montana was probably carried in the high-velocity (60–125 km/hr) wind layer at altitudes of about 10–13 km (fig. 335). This layer was transporting ash towards azimuths 093°–101° (1020 PDT at Spokane according to U.S. National Meteorological Service). By 1600, these high-velocity winds had shifted northeastward, toward azimuths 079°–087° (fig. 335). This shift in wind direction apparently is the cause of the axis of the earlier, dark ash being offset to the south of the axis of the later, light-colored ash (fig. 340). During late morning and afternoon of May 18, however, the slower low-level wind was consistently more northeastward than was the high-level wind. At Spokane, velocities of low-level winds at altitudes 2,250–5,300 m were 30–60 km/hr. At 1020 they were toward azimuth 005°–070°, and at 1600 toward azimuth 048°–070°. These vectors 10°–90° north of the high-level wind vectors explain why the ash fell on the ground north of the observed airborne-ash plume.

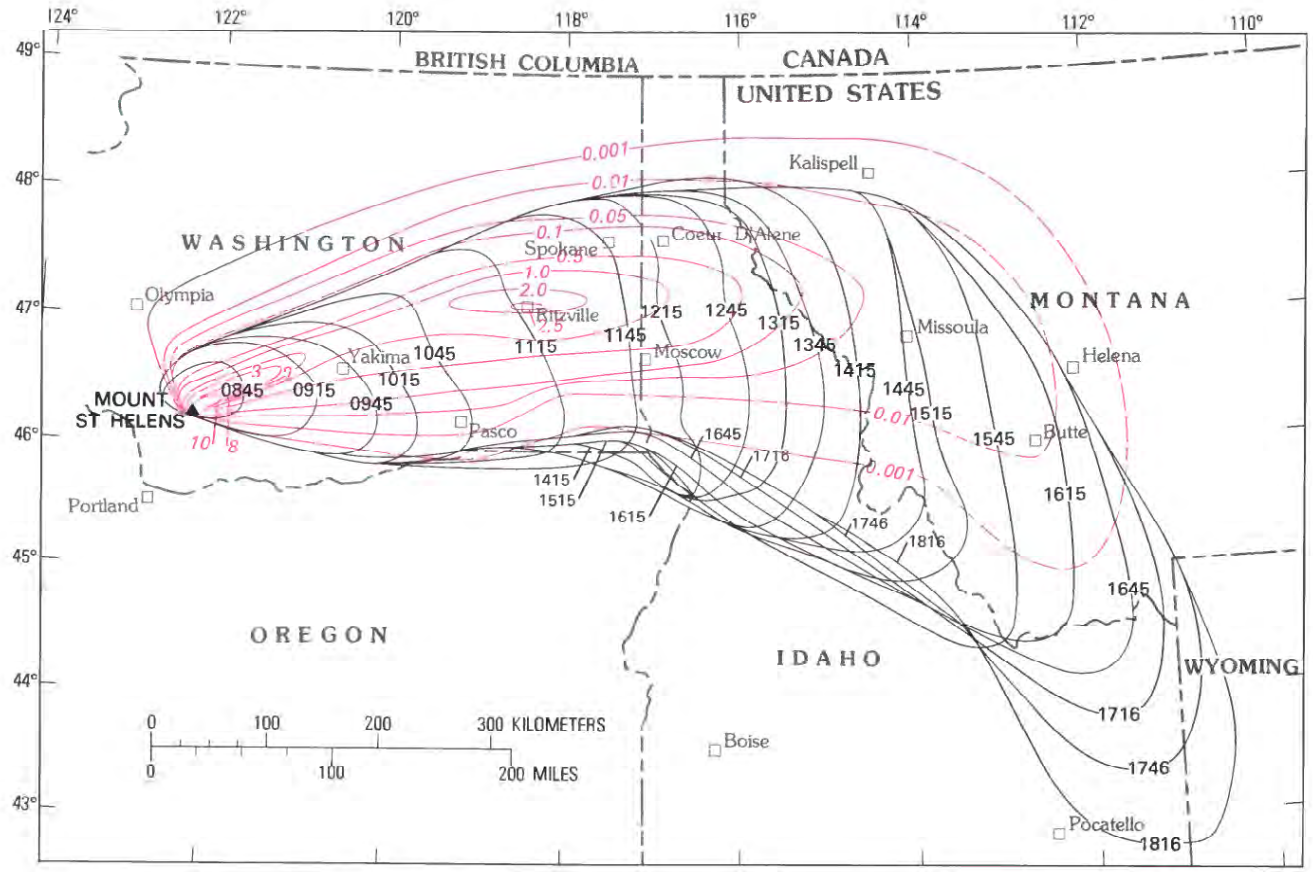

Figure 341.—Isochron and isomass maps compared. Black lines, isochrons of airborne-ash plume; red lines, isomass of fallen-ash lobe; and red dashed lines, inferred positions of isomass lines extended beyond area of control. Time in PDT. See figures 332, 338, and text for further explanation.

Winnowing of fine ash from the main body of the plume caused dusting and reduced visibility for tens of kilometers north of the northern boundaries of our isopach and isomass maps. The southern plume boundary, however, was quite sharp in south-central Washington. Within 50 km of Mount St. Helens, the southern margin of the air-fall lobe is marked by coarse, scattered pumice lapilli, but it contains no fine ash. Downwind in central Washington, eyewitnesses reported a sharp southern boundary to the falling ash, which was coarse- to medium-sand size. The fine ash was winnowed northward toward the axis of the air-fall lobe. Size analysis of ash samples confirms eyewitness observations. In Washington and northern Idaho, mean grain sizes on the south side of the downwind lobe are greater and size gradients are steeper than those on the north side (figs. 336, 342).

TOTAL VOLUME, MASS, AND AVERAGE BULK DENSITY FOR DOWNWIND ASH FROM THE MAY 18 ERUPTION

We estimated total, uncompacted bulk volume of downwind ash by measuring areas within each isopach contour of figure 336 using a planimeter. Each thickness increment was multiplied by its area, and volumes were summed. The total volume was multiplied by a correction factor[2] to compensate for unmeasured small volumes between the stepped increments and the curved surface of the ash lobe. The

[2]Total volume and mass values for the May 18 eruption (Sarna-Wojcicki and others, 1980) did not include this correction factor, which is calculated to be 1.33.

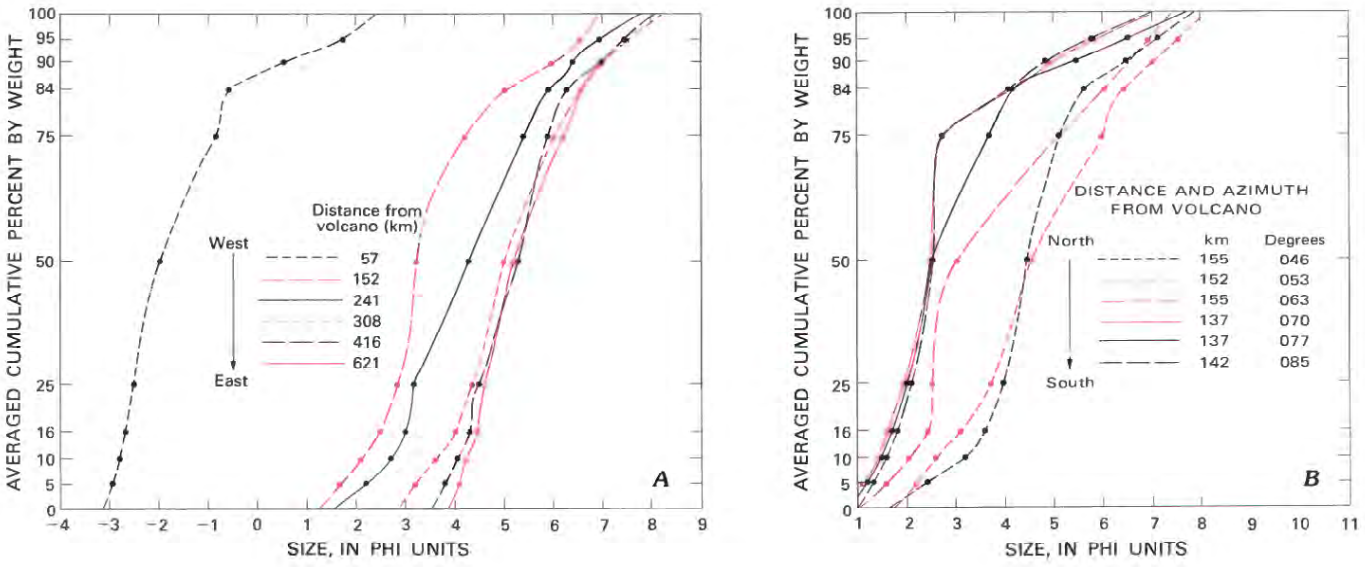

Figure 342.—Cumulative weight-percent curves of downwind ash at increasing distances from Mount St. Helens. A, Averaged curves. The curve representing the size distribution at 57 km downwind is from a single composite sample containing units A through D (Waitt and Dzurisin, this volume). The five curves representing greater downwind distances are averages of several samples from each of the five downwind traverses normal to the lobe axis (fig. 336). B, Cumulative weight-percent curves of downwind ash along a north-south traverse through Yakima, Wash.

estimated minimum total bulk volume of uncompacted downwind air-fall material (within the 0.5-mm isopach) is 1.1 km^3. This estimate is a minimum, because some of our thickness measurements were made after compaction.

We estimated the total mass of downwind ash in a similar way from figure 338. Total mass was between 4.9×10^{14} g and 5.5×10^{14} g. The greatest mass of air-fall ash fell in rather small areas, 4,000–40,000 km^2 (fig. 343); progressively smaller amounts fell in larger areas. The unmeasured mass beyond the 0.001 g/cm^2 isomass contour (fig. 343) is probably small. Part of the total mass, however, remained suspended and was transported beyond our study area; some of the finest dust and aerosol will remain suspended for several years (Symons, 1888). Our mass estimate is consequently a minimum. On the basis of analogy with previous eruptions and of graphic estimates of total air-fall volumes, Rose and Hoffman (1980) suggested that as much as 75 percent of the air-fall volume and 40 percent of the mass are outside the 2.5-mm isopach (fig. 336). An average bulk density of 0.45 g/cm^3 for the downwind lobe was calculated by dividing the total mass by the total uncompacted volume. If our initial uncompacted thicknesses are low, this value would be a maximum estimate of average initial uncompacted density.

We have calculated a range of solid-rock volumes that correspond to the mass of downwind ash. Although the density of solid unfractured dacite of the former volcano summit would have been about 2.8 g/cm^3, the material probably consisted of fractured and partly vesiculated rock as well as magma. We consequently assume that if the density of rock and magma before eruption is between 2.0 and 2.6 g/cm^3, then the equivalent in-place rock volume is between 0.20 and 0.25 km^3. The volume missing from the mountain after the eruption of May 18, calculated from preeruption and posteruption topographic maps, is 2.7 km^3 (Moore and Albee, this volume). Most of the missing volume must be in the debris avalanche, mudflows, and directed-blast deposits, whereas only a small fraction was erupted into and deposited by the downwind plume.

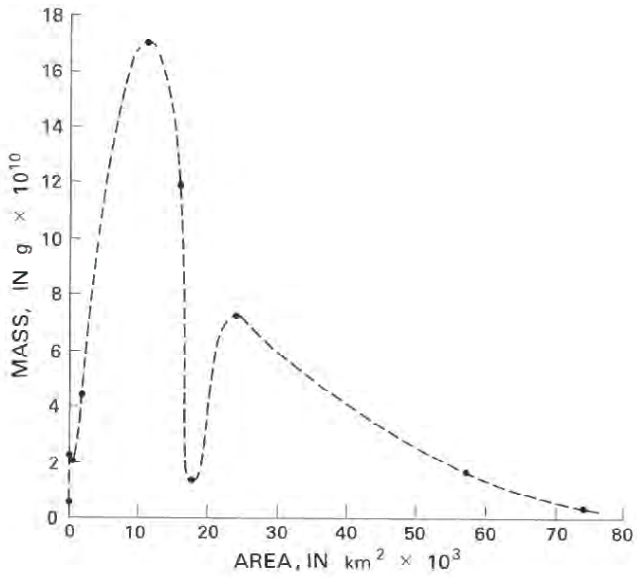

Figure 343.—Mass of downwind ash as a function of the size of the area covered. Areas bounded by isomass lines in figures 338 and 341 were planimetered, and the mass associated with each area increment plotted against the corresponding associated measured area increment.

AREAL DISTRIBUTION, THICKNESS, AND MASS OF ASH FROM THE FIVE MAJOR ERUPTIONS AFTER MAY 18

Eruptions from Mount St. Helens on May 25, June 12, July 22, August 7, and October 16–18 were considerably smaller in mass and volume than that of May 18. Distribution patterns from those eruptions, together with that of May 18, are instructive for anticipating areal extent of ash from future eruptions and for interpreting transport and dispersal patterns of ancient volcanic ashes.

Beyond 20 km from the volcano, the air-fall ash from the May 25 eruption was distributed over a 140° sector from the volcano, from azimuths 180°–320° (fig. 344). This wide distribution is a consequence of divergent wind directions at different altitudes above the volcano. The fast, higher level winds between altitudes 5,500 and 15,000 m blew toward the northwest (fig. 344). A layer of ash about 0.3–0.5 mm thick covered Aberdeen, Wash., about 150 km to the northwest. Traces of fine dusting were reported throughout much of the Olympic Peninsula, to distances of as much as 240 km to the northwest. The slower, lower level winds carried ash to the west, southwest, and south. Longview, Wash., 55 km west of the volcano, received 1–2 mm of ash, and Vancouver, Wash., about 75 km to the southwest, about 0.3 mm of ash. A distal thickness maximum similar to that near Ritzville, Wash., during the May 18 eruption appears 70–80 km northwest of Mount St. Helens (fig. 344).

Bulk volume for the May 25 eruption is 0.03 km^3 and total mass is 0.42×10^{14} g, giving an uncompacted average bulk density of 1.03. The equivalent in-place rock volume prior to eruption is between 0.016 and 0.022 km^3, or about 0.08 that of the May 18 eruption.

The air-fall ash distribution of the June 12 eruption is complicated, and probably is an effect of different wind directions at different altitudes (fig. 345). Wind vectors on June 12 were within a 90° arc, toward azimuth 150°–240° (fig. 345, inset). Thickness and mass were measured as far southwest as Vancouver, but farther downwind only thickness was measured. Data from nearby sites were used to estimate mass at sites where only thicknesses were measured. Airborne observers at an altitude of 5,000 m noted that ash was transported to the south, southwest, and west from the volcano. Ash distribution on the ground (fig. 345), however, indicates that low-level winds within 50 km of the volcano carried ash within a wide sector between azimuth 120° and 220°. Higher level winds at altitudes of about 7,500–12,000 m transported ash toward the southwest within a sector between azimuth 225° and 240°. Massive fallout from this cloud formed a distal thickness maximum about 45 km southwest of Mount St. Helens. Fine ash, which remained suspended at lower altitudes near St. Helens, Oreg., is inferred to have been transported to the south and southeast by lower level winds apparently localized along the Columbia River. Fine dusting, however, was reported farther south. The mass of material erupted on June 12 was about the same as that erupted on May 25 (table 66).

Thickness measurements of ash from the eruptions of May 25 and June 12 were of wet ash; consequently, thicknesses were less than if the ash had been dry. Average initial uncompacted bulk densities calculated from total volume and mass are 1.03 and 1.25 g/cm^3, respectively, for the two eruptions.

The eruption of July 22, like that of May 18, occurred on a fair day, and ash was carried to the northeast. Data for areal distribution and thickness of this ash are sparse beyond 135 km northeast of Mount St. Helens. Beyond several tens of kilometers from the

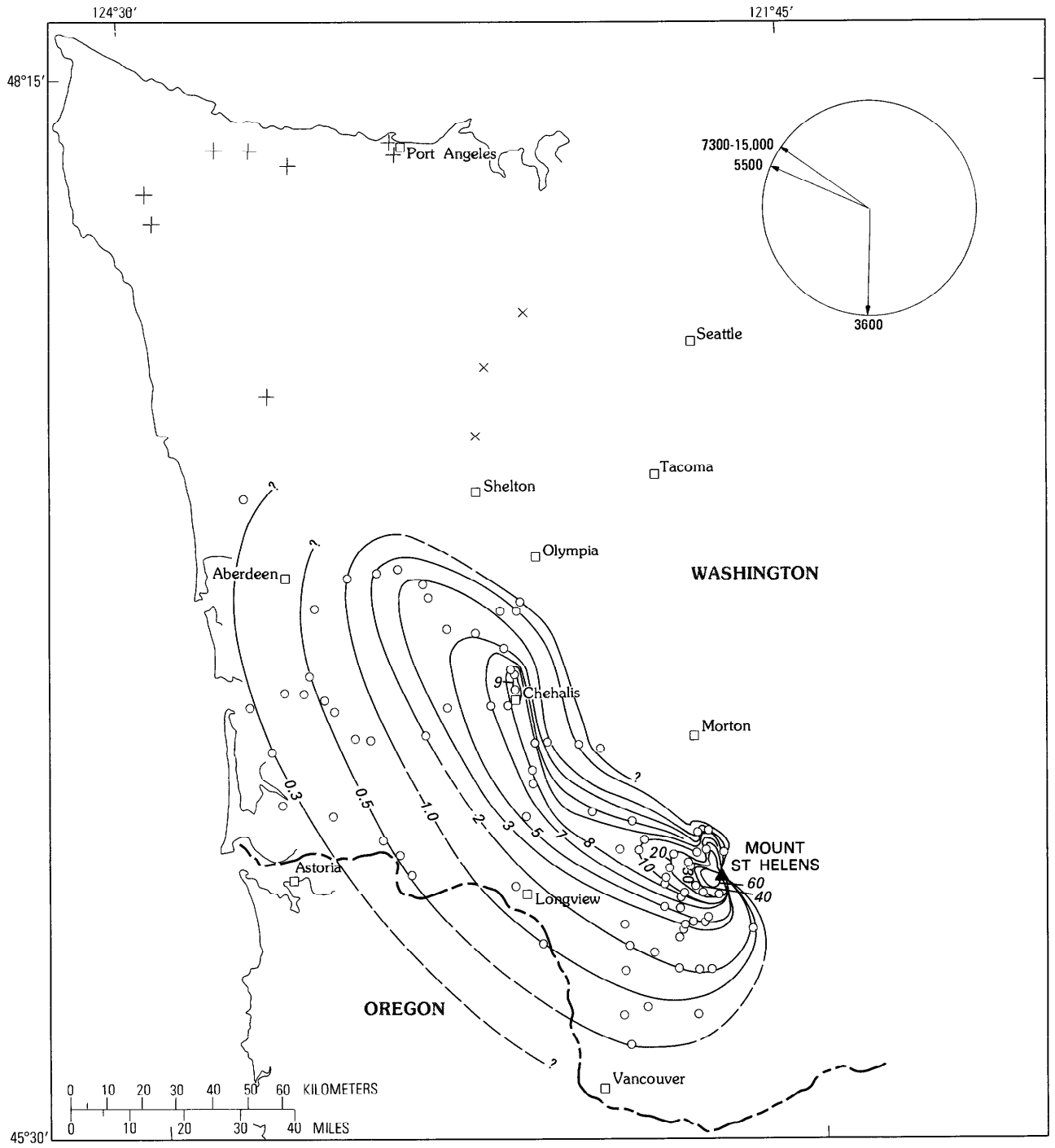

Figure 344.—Isopach map of air-fall ash of May 25. Ash thickness in millimeters. Circle, measureable amount of ash observed; +, light dusting or trace amount of ash observed; x, no ash was observed. Contour dashed where beyond control area. Circular diagram shows predicted wind directions for selected altitudes (in meters) near Mount St. Helens. Arrows point in the direction wind blew. Data are from U.S. National Weather Service. Data north and west of Chehalis, Wash., from James Beget.

Table 66.—Mass, volume, bulk density, and area covered by the 0.1-g/cm² isomass contour for downwind ash erupted from Mount St. Helens, March 27 through October 18.

	Early phase[1]	May 18	May 25	June 12	July 22	August 7	October 16–18
Total mass, x 10^{14} g	0.008	4.88	0.42	0.45	0.04	0.01	0.007
Volume, uncompacted, bulk km^3	[2].0006	1.10	.031	.027	[3].004	.0008	.0005
Volume, in-place rock, km^3 using density 2.6 g/cm^3	.0003	.20	.016	.017	.001	.0005	.00025
Calculated average uncompacted bulk density, g/cm^3	[2]1.25	.45	1.03	1.25	[3].50	1.25	1.29
Area covered within the 0.1-g/cm^2 isomass contour, in km^2	340	57,372	6,751	14,190	513	17.7	5.8

[1]Early premagmatic eruptions, March 27–April 17. Does not include some minor eruptive activity between April 17 and 22 and May 7–14.

[2]Thickness measurements were not reliable, or ash layers were too thin. Uncompacted density of 1.25 g/cm^3 was used, comparable to wet-ash values of June 12 eruption (see text).

[3]Ash too thin to measure at most sites. Uncompacted density of 0.5 g/cm^3 was used, comparable to dry-ash values of May 18 eruption (see text).

volcano, the ash was too thin to measure, and measurements only for mass per area were made (fig. 346). Near the volcano, the axis of the air-fall ash lobe trended about 060°, almost directly atop the May 18 axis, but whereas the axis of the May 18 lobe turned more eastward near Yakima, Wash., the July 22 air-fall lobe swung more northward. Mass values beyond Yakima are scattered and cannot be contoured reliably. Mass measurements near the Idaho-Canada border, about 490 km to the northeast, were higher than values in intervening areas. These variations in thickness may result from strong low-level winds that blew throughout the day and disturbed the ash, or the higher values downwind may represent distal thickness maximums similar to those described for the previous three eruptions.

As occurred in the earlier eruptions, the lobe deposited on July 22 had a pronounced asymmetry, which probably resulted from divergent wind directions at different altitudes. Faster, high-level winds were directed toward a sector from azimuth 043°–055°, but lower level winds were directed to about 068° (fig. 346, inset). Thus the northwest boundary of the plume was fairly sharp and the mass gradient was fairly steep for proximal areas, but the southeastern boundary was more diffuse and the mass gradient tailed off gradually. We estimate a mass of 4×10^{12} g for the July 22 eruption, assuming a configuration for the 0.0004-g/cm^3 isomass contour as shown in figure 347. The air-fall mass estimated for the July 22 eruption was about 122 times smaller than that for the May 18 eruption. If we assume an uncompacted bulk density of about 0.50 g/cm^3 for ash from this eruption, which is similar to that of the May 18 eruption which also occurred on a fair day, then the uncompacted bulk volume of ash from this eruption is about 0.004 km^3, and the equivalent in-place rock volume prior to eruption is about 0.001 km^3 (fig. 347, table 66).

Distribution patterns for the eruptions of August 7 and October 16–18 (figs. 348, 349) are multilobed, which most likely reflects shifts in wind directions between successive eruptive pulses. Three major pulses, for instance, were recorded during the August 7 eruption, which may correspond to the three lobes observed in the ash-distribution pattern. Distal thickness maximums are also observed for both the August and the October eruptions. Four distal maximums are observed for the eruption of October 16–18, in which five separate eruptive pulses were noted. Analyses of ash-distribution patterns and their correlation with wind direction and altitude for the later eruptions are still in progress.

Erupted mass and volume for the six major eruptions of 1980 from Mount St. Helens declined roughly exponentially with time and leveled off somewhat between the last two eruptions (fig. 350). Differences in mass and volume between the first and last eruption are three orders of magnitude.

VOLUME OF DOWNWIND ASH FROM THE MAY 18 ERUPTION COMPARED WITH VOLUMES FROM PREVIOUS ERUPTIONS OF MOUNT ST. HELENS

One way to compare the magnitude of the May 18 eruption with magnitudes of previous eruptions of Mount St. Helens is to compare the volumes of their respective tephra deposits. Evidence for many of the older tephra layers from Mount St. Helens, however, is fragmentary and volumes cannot be accurately measured. Both thickness data and volume estimates for several historic eruptions from other volcanoes, however, are available. We have plotted curves of maximum air-fall thickness against distance for each of these historic eruptions. At distances of about 25–100 km downwind, the slopes of these curves are roughly parallel, and thickness increases directly with volume. Next, we plotted the maximum thicknesses of the historic tephra layers (at arbitrarily chosen distances of 50 and 100 km from their vents) against the volume of each eruption (fig. 351). Using thick-

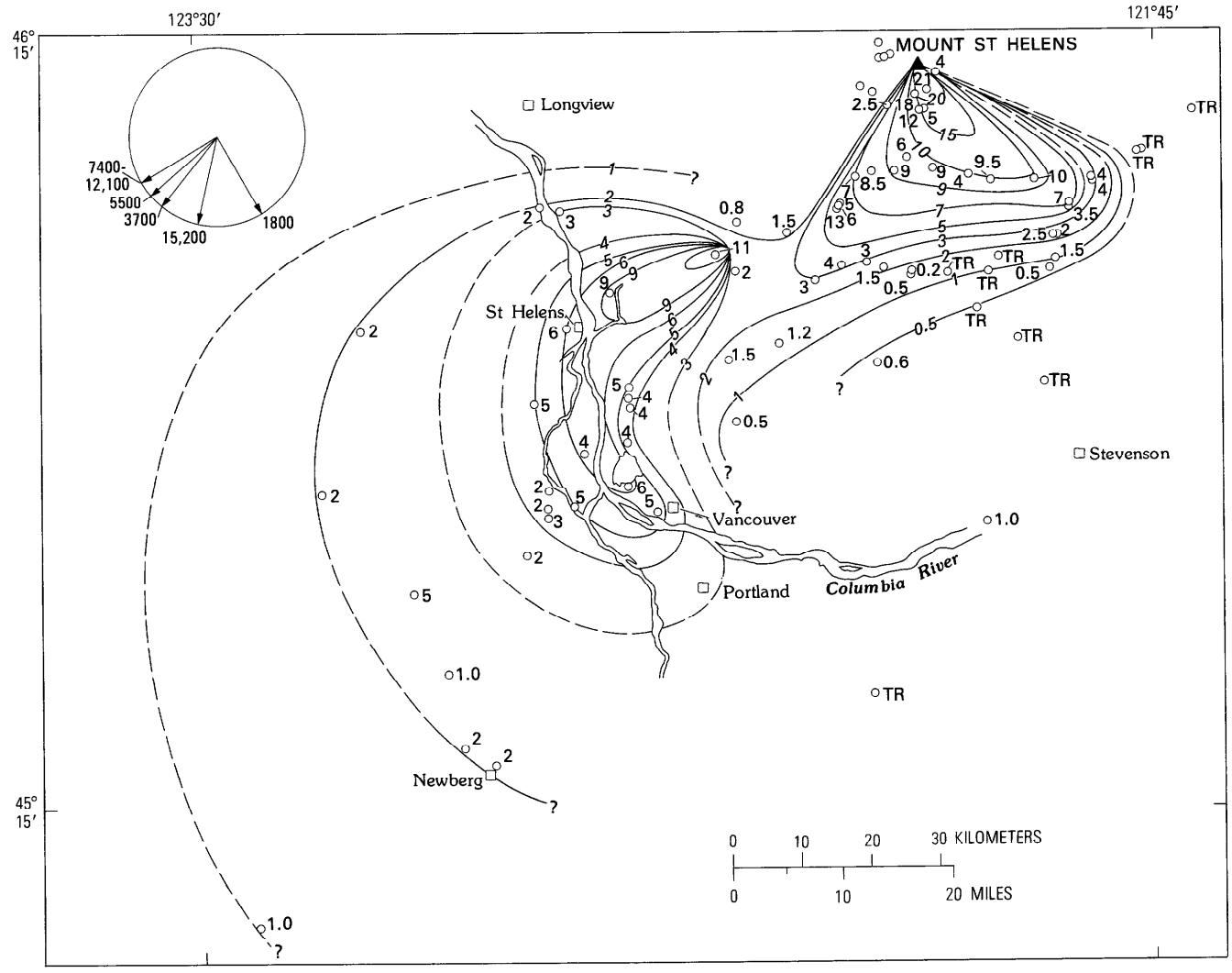

Figure 345.—Isopach map of air-fall ash of June 12. Ash thickness in millimeters. Circle, observation site with measured thickness (these are given because thickness values are scattered, and some appear anomalous); TR, trace; dashed lines, beyond control area. Circular diagram shows predicted wind directions for selected altitudes (in meters) near Mount St. Helens. Arrows point in the direction wind blew. Data are from U.S. National Weather Service. Data from sites southwest of Columbia River, from C.F. Kienle. Data for some stations south of Mount St. Helens, from Carolyn Driedger and Jerry Kendall.

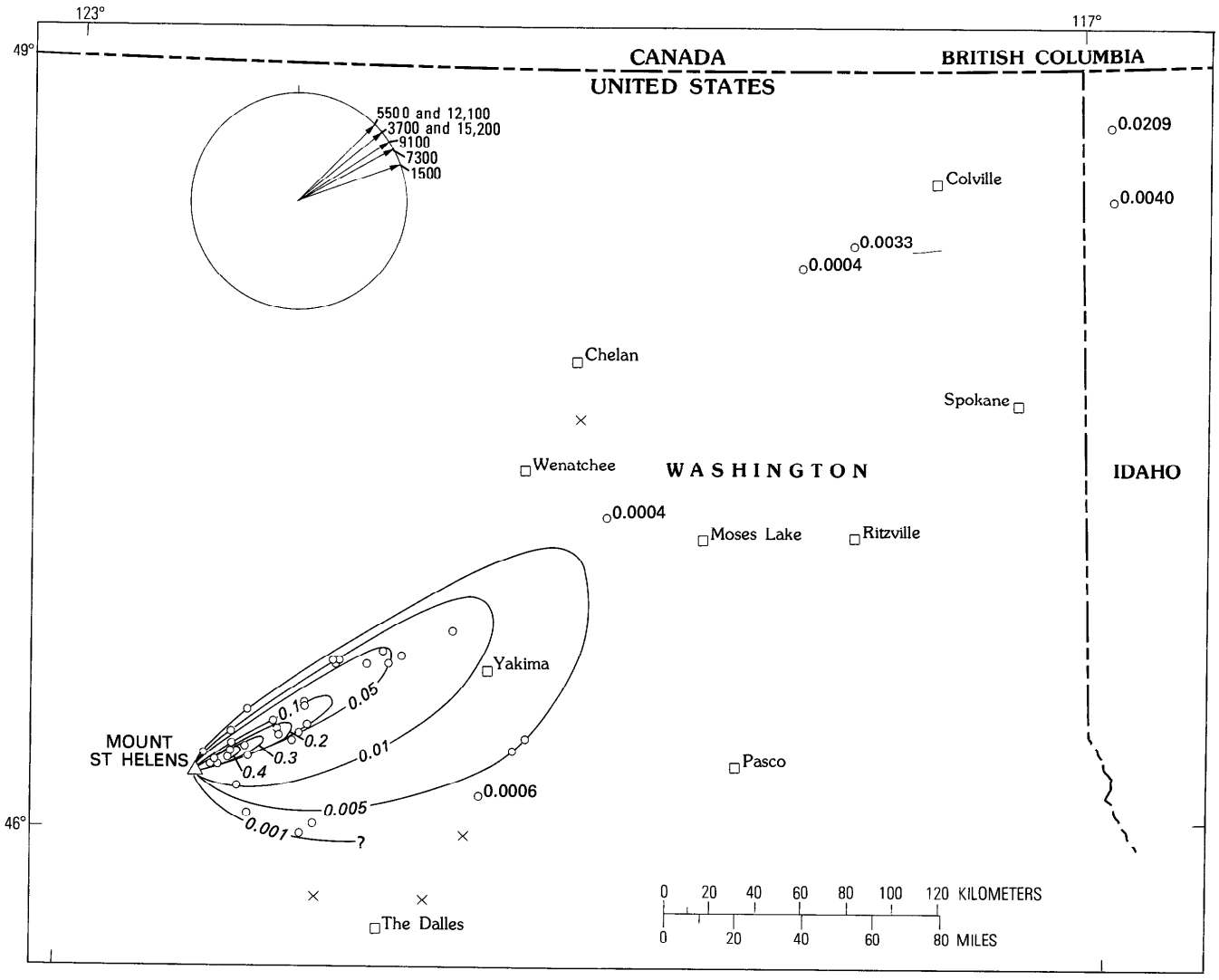

Figure 346.—Isomass map (mass per unit area, in g/cm²) map of air-fall ash of July 22. Circle observation site; x, no ash observed. For sites beyond the contoured area numbers represent mass in g/cm². Circular diagram represents predicted wind directions for selected altitudes, in meters, in the vicinity of Mount St. Helens. Arrows point in the direction toward which the wind blew. Data are from the U.S. National Weather Service. Data for distal sites in central Washington from M. P. Doukas. Data for sites in vicinity of Colville, Wash., from Brian Atwater and Kenneth Fox. Data from northwestern Idaho, from Fred Miller.

ness data for some of the previous eruptions of Mount St. Helens (Crandell and Mullineaux, 1978) and curves from figure 351, we estimate that the 1842 layer of Mount St. Helens had a volume of about 0.03 km³, that layer T (erupted about A.D. 1800) had a volume of between 0.3 and 0.4 km³, and that layer Yn (erupted about 4,000 B.P.) had a volume of about 4.5–5 km³, compared to the 1.1 km³ volume of the May 18 eruption. In this method of comparison, volumes of broad, diffuse lobes or of lobes with distal maximums such as that of May 18 will be underestimated, but volumes of sharp, narrow lobes will be overestimated; consequently, these estimates are rough, probably within a factor of two of the actual

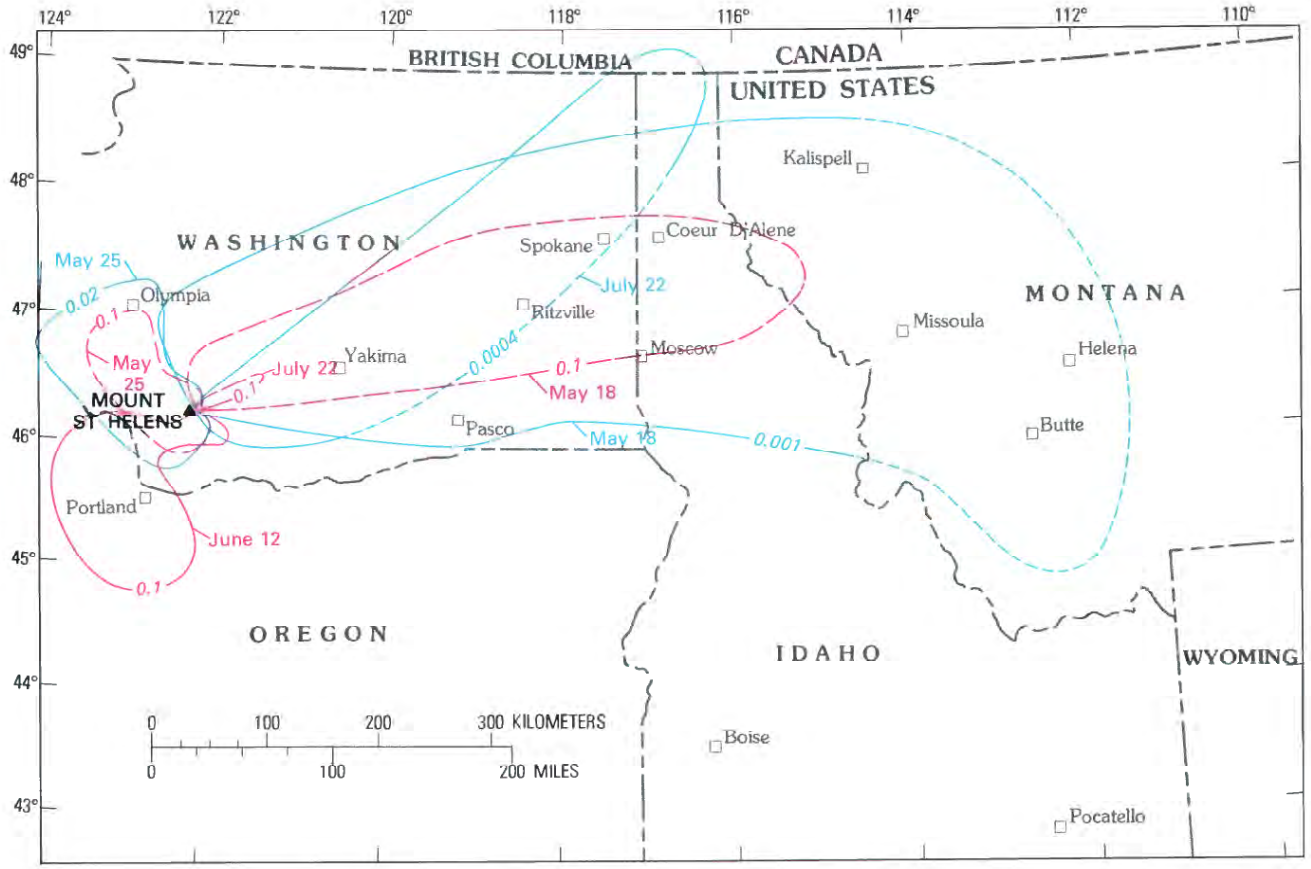

Figure 347.—Comparison of isomass maps for the first four eruptions of 1980. Numbers on contours represent mass-per-unit area, in g/cm². The 0.1-g/cm² contour is shown for each of the four eruptions. One contour is shown for the June 12 eruption; two contours are shown for the May 18, May 25, and July 22 eruptions.

volumes.

Another method of estimating the relative magnitude of the May 18 eruption is to compare the area covered by a certain isopach with the areas of the same isopach of previous eruptions. The 20-cm isopachs for air-fall ejecta of five previous eruptions of Mount St. Helens (Crandell and Mullineaux, 1978) are compared with the 20-cm isopach of air-fall deposits of the May 18 eruption (fig. 352). We have also estimated the minimal volumes within the 20-cm isopach contours of each of these eruptions by multiplying the measured areas by 20 cm (table 67). The area covered by 20 cm or more of air-fall tephra from the May 18 eruption is very small, about 16.2 km² (dark pattern of fig. 352), compared to previous large tephra eruptions of Mount St. Helens. In this comparison, however, another factor needs to be considered in addition to errors resulting from differences in shapes of different lobes: the magnitude of the May 18 eruption cannot be assessed on the basis of volume of air-fall tephra alone, because much of the energy of the eruption was spent on the initial directed blast. The blast contained much fragmented older rock that had made up the volcanic edifice, together with lesser amounts of other pumice and juvenile rock. Consequently, much of the initial energy of the eruption was expended on moving dense, solid rock laterally, rather than propelling light pumice and ash vertically. Volume of air-fall tephra might have been considerably greater if the north slope of the mountain had not failed and triggered the directed blast. If the blast deposit and air-fall-ash areas are considered together,

Table 67.—Area and volume of air-fall ash of the May 18 eruption compared with those of five older eruptions from Mount St. Helens.

[Data for older eruptions from Crandell and Mullineaux, 1978; see fig. 352]

	May 18 (air fall)	May 18 (total)[1]	Layer T	Layer Wn	Layer We	Layer Yn	Layer Ye
Area within the 20-cm isopach, km^2	16.2	276	108	534	138	1698	120
Minimal volume within 20-cm isopach, km^3	0.003	0.06	0.02	0.11	0.03	0.34	0.02
Relative volume, if May 18 (air fall)=1	1	20	6.7	37	10	113	6.7

[1]Includes directed-blast deposit (units A_1 and A_2) as well as air-fall tephra. Does not include debris-avalanche or mudflow deposits.

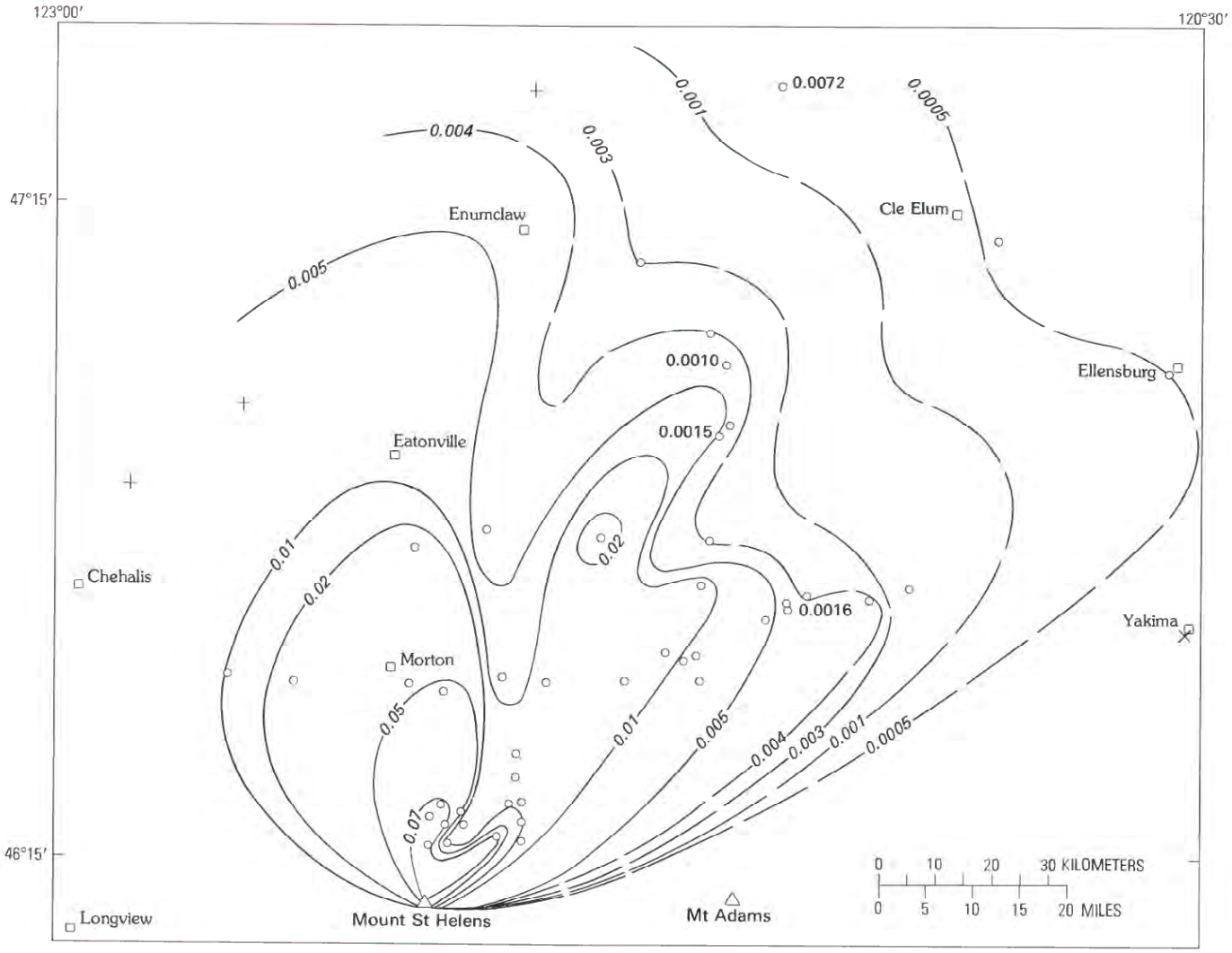

Figure 348.—Isomass map (mass per unit area, in g/cm²) of air-fall ash of August 7. Numbers adjacent to individual sites are mass-per-area values, which are anomalously high or low relative to adjacent contours. Circle, observation site; +, light dusting of ash; x, no ash observed. Contour dashed where inferred beyond control area. Samples collected by M. P. Doukas, R. B. Waitt, Jr., and J. A. Barker.

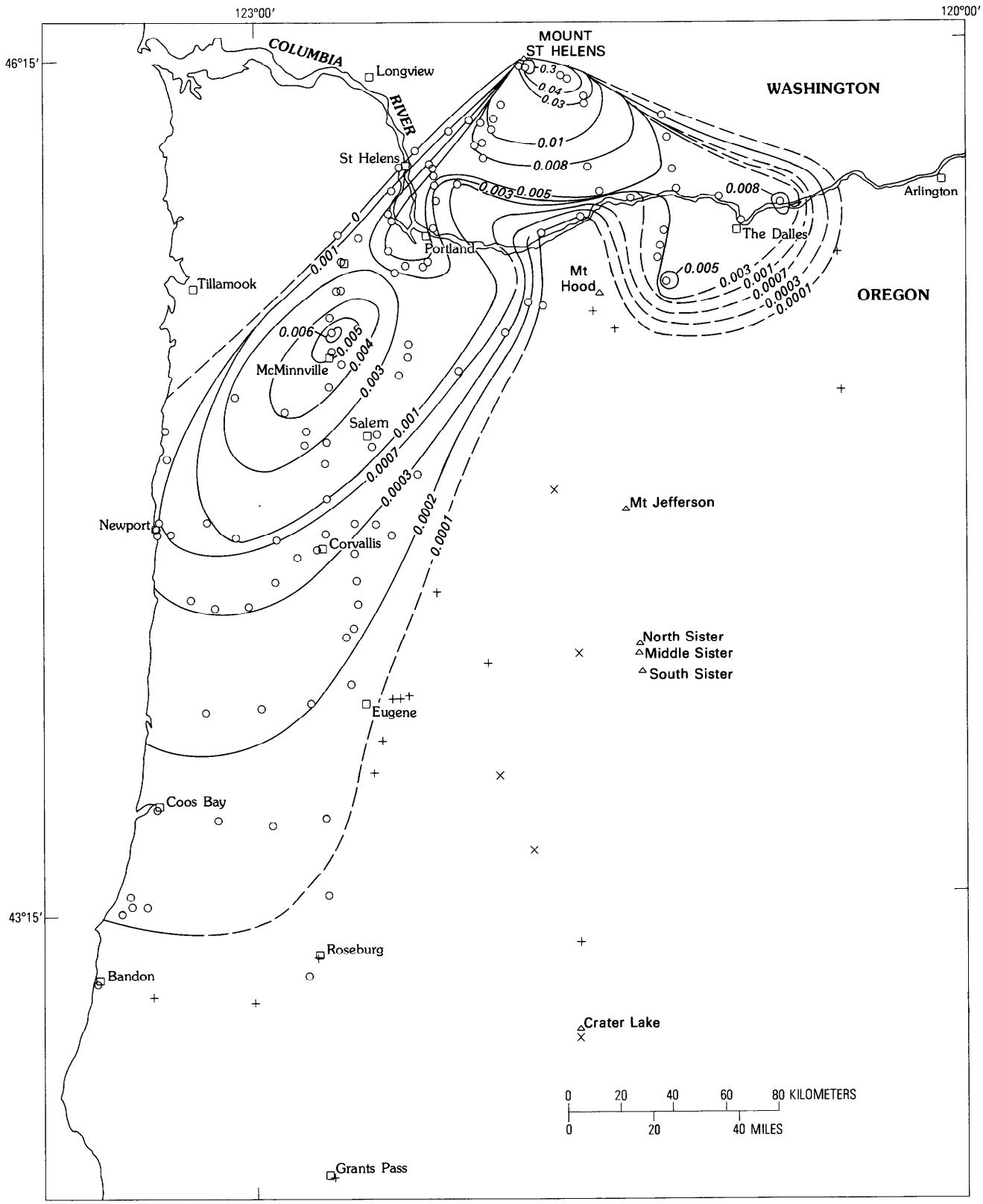

Figure 349.—Isomass map (mass per unit area, in g/cm²) of air-fall ash of October 16–18. Circle, observation site; +, light dusting of ash; x, no ash observed. Contour dashed where inferred beyond control area. Samples collected by Evelyn Newman, Robert Mark, Carol Price, and Susan Shipley.

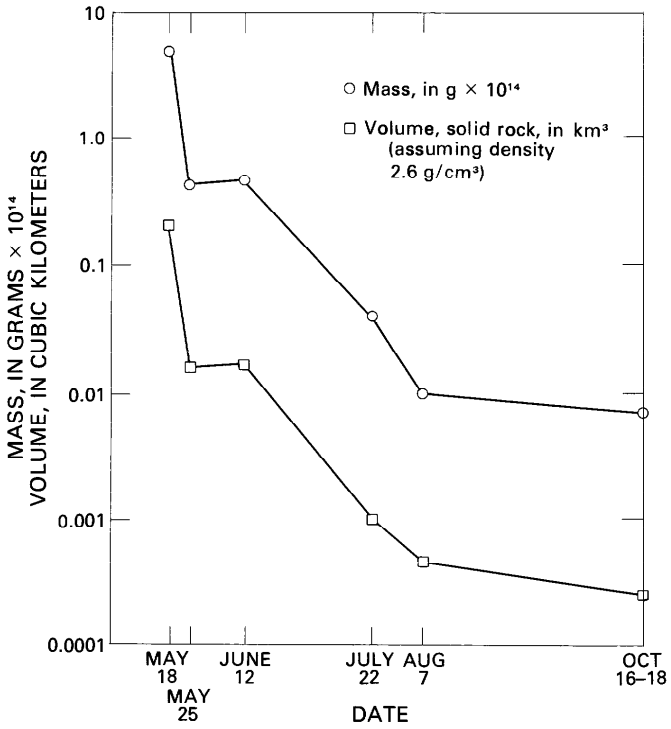

Figure 350.—Mass and volume of air-fall ash from six 1980 eruptions of Mount St. Helens.

however, the area covered by the 20-cm isopach is larger (light pattern of fig. 352), and the minimal volume within that isopach is about 0.06 km³ (table 67). Thus, if we rank the eruption of May 18 on the basis of air-fall volume alone, it would be smaller than five of the most recent large tephra eruptions of Mount St. Helens (table 67); but if the directed-blast deposit as well as air-fall tephra is considered in the comparison, the May 18 eruption would be equal to or somewhat greater than the eruptions that produced layers T, We, and Ye, but smaller than the eruptions that produced layers Wn and Yn (table 67).

SUMMARY

During the current episode of activity the eruption of May 18 produced by far the largest volume of material and covered the largest area (table 66); it accounted for about 84 percent of the total mass of ash erupted since activity started, 83 percent of the estimated volume, and about 93 percent of the uncompacted bulk volume. The eruption of May 18 covered 72 percent of the total area blanketed by the 1980 eruptions if the 0.1-g/cm² isomass contour is used as a basis of comparison (fig. 347). Total volume, mass, and area covered by each of the six magmatic eruptions have decreased markedly and, with the exception of the May 25 eruption, systematically with time. The volume of air-fall tephra erupted on May 18 is the smallest when compared to the volumes of previous major eruptions from Mount St. Helens, but the volume is intermediate if the directed-blast deposit is included with the air-fall tephra.

None of the ash lobes produced by the six magmatic eruptions of 1980 is truly symmetrical; some of them, like those of May 25, June 12, August 7, and October 16–18, have complicated distribution patterns. These characteristics of ash distribution are effects of variations in wind velocity and direction with altitude, combined with characteristics of the vertical eruptive column. Similar factors probably have affected distribution of ancient ashes. Increase in thickness downwind toward distal thickness maxima could be misinterpreted in the stratigraphic record as thickening toward a source. The observed ash distributions for these modern eruptions not only represent a predictive tool for determining possible distribution patterns for future eruptions of active volcanoes, but also are models for interpreting dispersal patterns of ancient ashes.

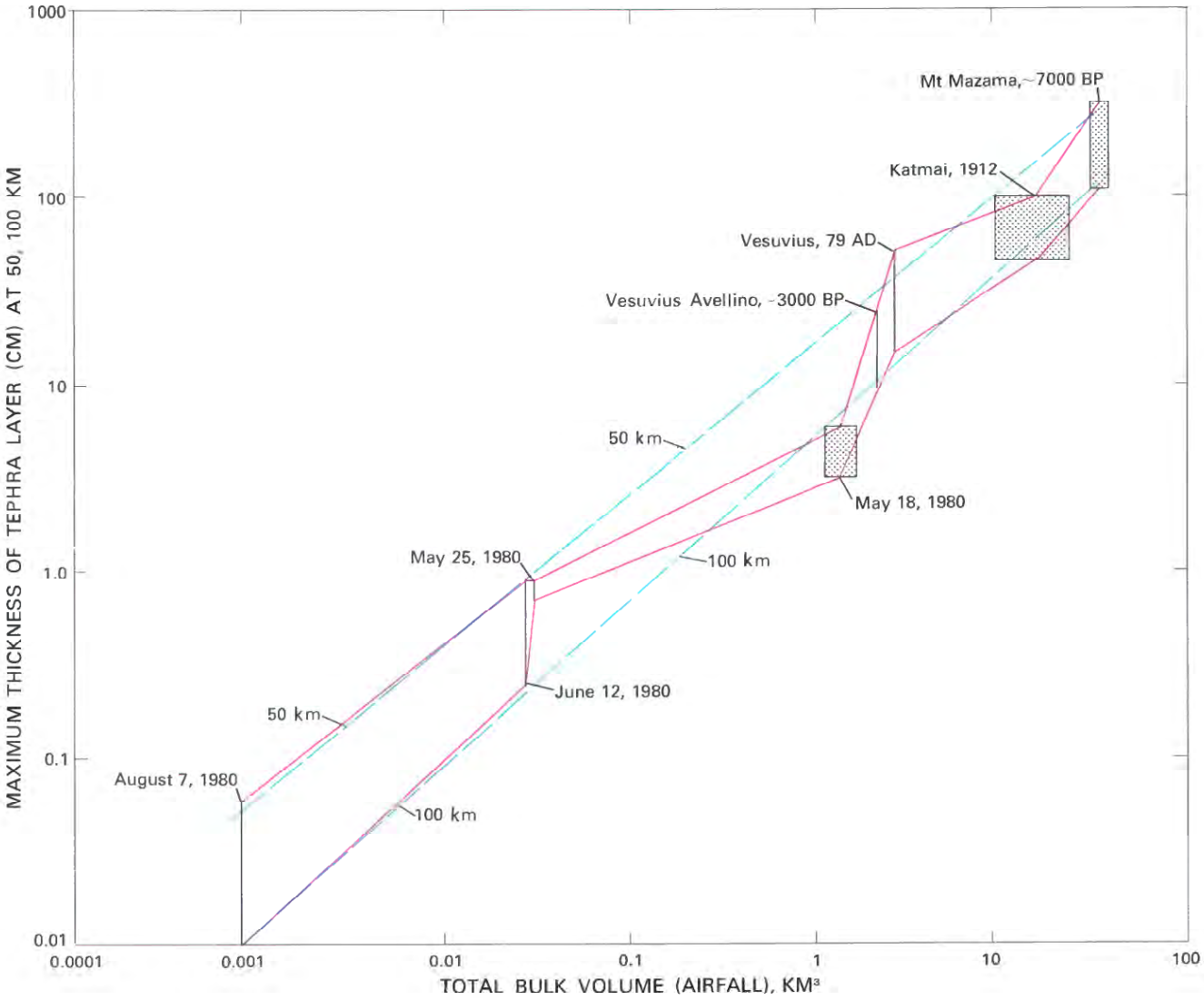

Figure 351.—Maximum thicknesses of air-fall tephra layers at distances of 50 and 100 km from the volcano (vertical black lines), plotted against estimated volumes of erupted tephra for Mount St. Helens, Mount Mazama (Williams, 1942; Williams and Goles, 1968), Katmai (Wilcox, 1959; Curtis, 1968), Vesuvius A.D. 79 (Lirer and others, 1973), and Vesuvius Avellino (Lirer and others, 1973) (red lines). Blue lines are visually averaged through the data points. Shaded areas indicate volume-to-thickness ratio uncertainties.

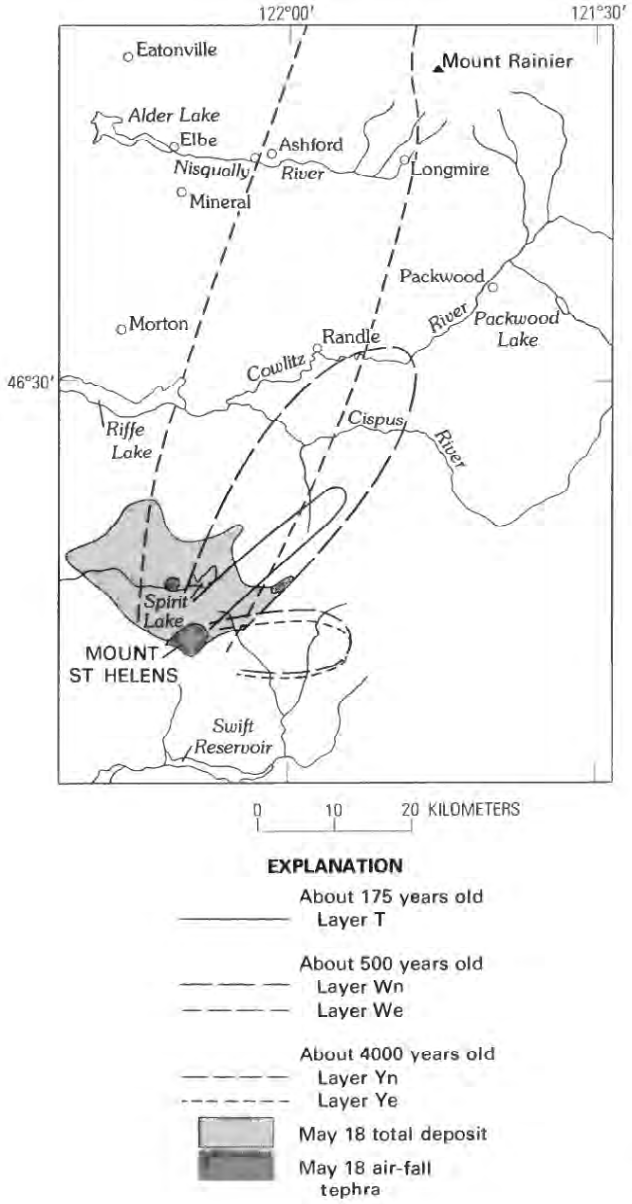

Figure 352.—Areas covered by 20 cm or more of tephra during five relatively large pre-1980 tephra eruptions, compared with air-fall tephra of the May 18 eruption and total deposits of 20 cm or more from May 18 eruption excluding debris avalanche, mudflows, and pyroclastic pumice-ash flow. Figure modified from Crandell and Mullineaux (1978, fig. 2).

REFERENCES CITED

Crandell, D. R., and Mullineaux, D. R., 1978, Potential hazards from future eruptions of Mount St. Helens Volcano, Washington: U.S. Geological Survey Bulletin 1383-C, 26 p.

Curtis, G. H., 1968, Stratigraphy of ejecta from the 1912 eruption of Mount Katmai and Novarupta, Alaska, *in* Coats, R. R., Hay, R. L., and Anderson, C. A., eds., Studies in volcanology: Geological Society of America Memoir 116, p. 153-210.

Danielson, Edwin, 1980, Mount St. Helens plume dispersion based on trajectory analysis [abs.]: NASA Symposium on Mount St. Helens Eruption, 1980, Washington, D.C., Abstract Digest, p. 21.

Hooper, P. R., Merrick, I. W., and Laskowski, E. R., 1980, Composition of the Mount St. Helens ashfall in the Moscow-Pullman area on May 18, 1980: Science, v. 209, no. 4461, p. 1125–1126.

Larsson, Walter, 1937, Vulkanische Asche vom Ausbruch des chilenischen Vulkans Quizapú (1932) in Argentina gesammelt—Eine Studie über äolische Differentiation: Uppsala University Geological Institution Bulletin, v. 26, p. 27–52.

Lirer, L., Pescatore, T., Booth, B., and Walker, G. P. L., 1973, Two Plinian pumice-fall deposits from Somma-Vesuvius, Italy: Geological Society of America Bulletin, v. 84, p. 759–772.

Rose, W. I., Jr., and Hoffman, M. F., 1980, Distal ashes of the May 18, 1980, eruption of Mount St. Helens [abs.]: EOS (Transactions American Geophysical Union), v. 61, no. 46, p. V28.

Sarna-Wojcicki, A. M., Shipley, Susan, Waitt, R. B., Jr., Dzurisin, Daniel, Hays, W. H., Davis, J. O., Wood, S. H., and Bateridge, Thomas, 1980, Areal distribution, thickness, and volume of downwind ash from the May 18, 1980, eruption of Mount St. Helens: U.S. Geological Survey Open-File Report 80-1078, 11 p.

Symons, G. J., F. R. S., ed., 1888, The eruption of Krakatoa and subsequent phenomena, Report of the Royal Society: London, Harrison and Co., 494 p.

Wilcox, R. E., 1959, Some effects of recent volcanic ash falls with especial reference to Alaska: U.S. Geological Survey Bulletin 1028-N, p. 409–476.

Williams, Howel, 1942, Geology of Crater Lake National Park, Oregon: Carnegie Institution of Washington Publication 540, 162 p.

Williams, Howel, and Goles, Gordon, 1968, Volume of Mazama ash-fall and the origin of Crater Lake caldera: Oregon Department of Geology and Mineral Industries Bulletin 62, p. 37–41.

THE 1980 ERUPTIONS OF MOUNT ST. HELENS, WASHINGTON

PROXIMAL AIR-FALL DEPOSITS FROM THE MAY 18 ERUPTION—STRATIGRAPHY AND FIELD SEDIMENTOLOGY

By RICHARD B. WAITT, JR., *and* DANIEL DZURISIN

ABSTRACT

Proximal air-fall deposits of the May 18 eruption of Mount St. Helens comprise four principal stratigraphic units. In upward succession they are: gray sandy silt (part of unit A), pumice and lithic gravel (unit B), pale-brown sand and silt (unit C), and gray silt (unit D). From 20 to 60 km east-northeast of the mountain the entire air-fall lobe and the lobes of each unit thicken exponentially toward areas near the volcano. Layer A3, the air-fall component of unit A, thickens toward an apparent source area 15 km north of the volcano. Its content of vesicular gray dacite and scorched tree fragments shows that it is related to the directed blast (pyroclastic density flow) that began at 0833 PDT. Unit B thickens toward the central vent and clearly is the primary deposit of the plume from the central eruptive column. Four layers composing this unit are attributed to fluctuations in the height of the eruptive column in the morning and afternoon. Unit C thickens toward the ash-flow deposits west of Spirit Lake and is largely the deposit from ash clouds that rolled outward from and convected upward off ash flows on the north flank during the afternoon. It is also partly a distal air-fall deposit from phreatic vents that redistributed ash-flow material as secondary eruptive columns. Unit D, which thickens toward the central vent, resulted from the waning central column in the evening. This four-unit stratigraphy comprising more than 10 distinctive layers accumulated within 12 hr. Ancient multi-layered deposits from Mount St. Helens and other volcanoes may represent similar sets of discrete but nearly simultaneous events.

At distances of 10–100 km from the volcano, the entire May 18 air-fall lobe is similar in thickness to ancient pumice layer T (A.D. 1800), the thickest air-fall deposit of the early 19th-century eruptive episode of Mount St. Helens. Unit B of the May 18 air-fall lobe is half to one-fourth as thick as pumice layer T. Unit D, an order of magnitude thinner than pumice layer T, is similar in thickness to the A.D. 1842–43 lobe, the thickest deposit of the mid-19th-century activity. The May 18 unit-B deposit is an order of magnitude both thinner and finer grained than the thickest and coarsest Quaternary air-fall deposits from Mount St. Helens and other Cascade Range volcanoes.

INTRODUCTION

The eruption of Mount St. Helens on May 18, 1980, had several phases. Moments after the great north-side landslide at 0832 PDT, a directed blast (pyroclastic density flow) swept off the volcano and within minutes spread across and devastated a 500-km² area to the north (fig. 353). Between 4 and 10 min after the beginning of the blast (Rosenbaum and Waitt, this volume), a vertical eruptive column developed as high as 20 km and alternately waxed and waned throughout the morning and afternoon. From ash flows that descended the north flank during the afternoon, convecting clouds of elutriated ash drifted downwind. By late afternoon secondary phreatic vents that developed in the ash-flow deposits 7 km north of the central vent redistributed some of the ash-flow material by means of secondary vertical columns. By evening the central column had greatly subsided but continued to emit ash. During each of these phases of the eruption, ejected material was carried east-northeast and winnowed by the prevailing windstream.

Within a few days after the eruption, we had categorized the air-fall deposits 20–60 km downwind

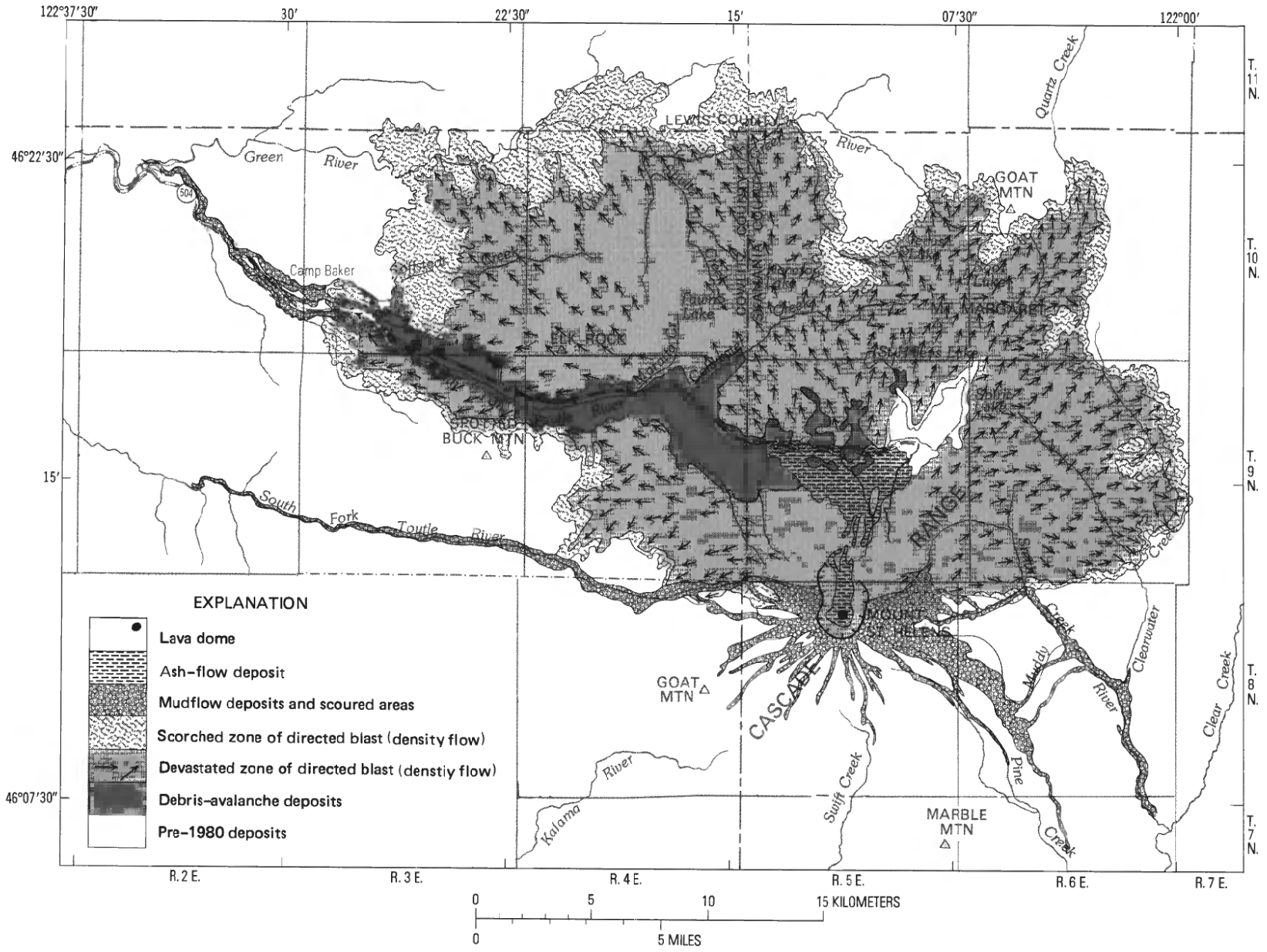

Figure 353.—Index map of Mount St. Helens area showing deposits and features of the 1980 eruptions. Geology modified from plate 1.

of the volcano into four units, designated from bottom to top as unit A (dark-gray sandy silt[1]), unit B (pumice and lithic gravel[1]), unit C (pale-brown sand to silt), and unit D (gray silt) (fig. 354*A*)[2]. This stratigraphy was followed toward the volcano, where between late May and late September these units were subdivided and developed into a comprehensive stratigraphy (fig. 354*B*). We report here on the stratigraphy and origin of air-fall deposits within 60 km of the volcano ("proximal area"). Sarna-Wojcicki, Shipley, and others (this volume) provide a comprehensive regional treatment of the air-fall deposits.

ACKNOWLEDGMENTS

This work has benefited from collaboration with colleagues in the U.S. Geological Survey. Judy A. Barker, Michael P. Doukas, and Susan Shipley assisted in the field in August and September. A few of the field data on the east and southeast were collected by Andrei Sarna-Wojcicki and Spencer Wood. Vicki L. Hansen collated numerical data from field notes and drafted the preliminary figures. Discussions with Andrei M. Sarna-Wojcicki and Susan Shipley, who have reduced regional data on the airborne plume, air-fall deposit, and geochemistry, have aided our understanding of the proximal air-fall deposits.

STRATIGRAPHY

The relatively straightforward four-unit stratigraphy of the broad area 20–60 km downwind of the volcano (fig. 354*A*) thickens considerably and becomes more complex closer to the volcano. At a distance of 20 km along the axis of the air-fall lobe, unit B is readily divisible into three layers. Closer to the volcano units A, B, and C are each similarly divisible into several layers. The composite proximal stratigraphic column (fig. 354*B*) shows the most complete stratigraphic sequence.

Isopach maps of air-fall units are based on about

[1]Standard Wentworth (1922) sediment-size terms are used to provide a distinct designation for each grain-size interval. Unit designations like "granule gravel," taken from Folk (1974), designate only median grain size of the deposit, and not rounding, sorting, or genesis of particles. Fuller explanation appears in Waitt (this volume).

[2]Units B and C of May 18 are not to be confused with tephra sets B and C that Mullineaux and Crandell (this volume) have designated in the ancient stratigraphy of the volcano.

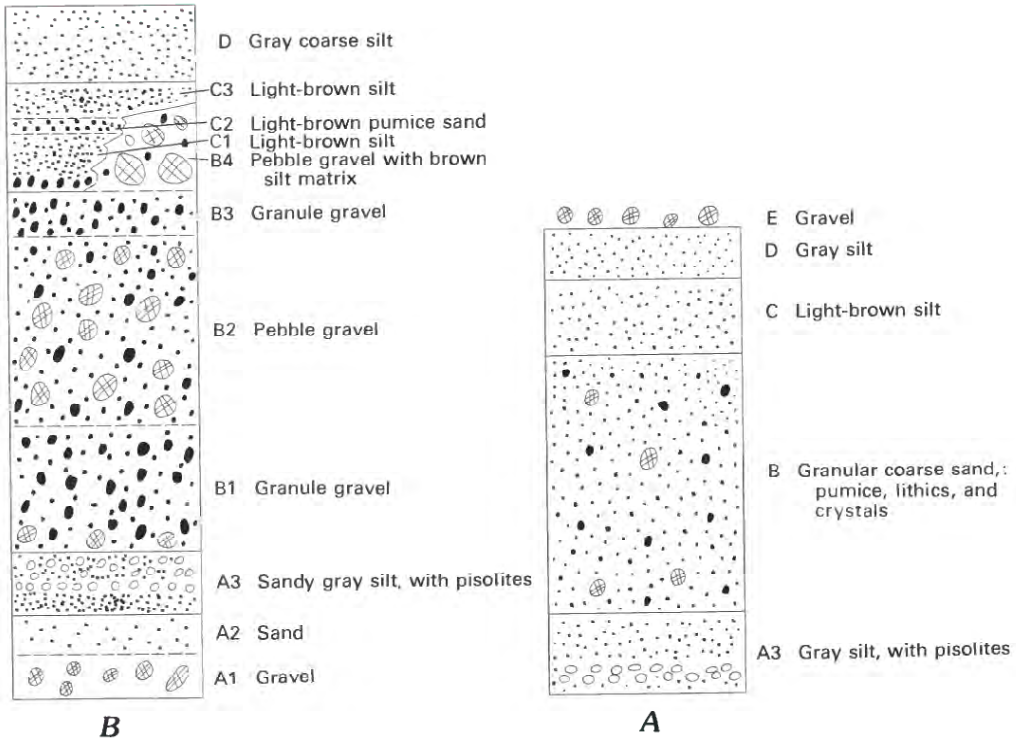

Figure 354.—Schematic stratigraphic columns of air-fall deposits from the May 18 eruption. A, column 40 km from volcano, differentiation by units (except for layer A3). B, composite column within 10 km of volcano, all distinct layers shown.

250 excavations scattered east to northwest of the volcano (fig. 353). The total-thickness isopach map of May 18 units shows a broad northward lobe and a sharp east-northeast lobe (fig. 355). These lobes are the deposit from two principal events of May 18: (1) a directed blast (pyroclastic density flow) that catastrophically swept 10–25 km to the north, northwest, and northeast and an attendant air fall extending another 30 km outward (Waitt, this volume); and (2) the vertical eruptive column and other events that ejected material high enough to enter the east-northeast windstream. All but roughly 2 cm (layer A3) of the northward lobe is the direct deposit of the blast (density-flow) event (layers A1 and A2) (figs. 258, 262 and 263). The east-northeast lobe comprises four overlapping air-fall units, mostly coarse air-fall pumice and lithic fragments from the central eruptive column (unit B). But the four units do not all emanate from exactly the same source area.

Beyond 5 km from the volcano, there is little local variation in thickness of the primary air-fall units within or among nontimbered areas. Near the trunks of living conifers, however, air-fall material is somewhat thinner because of outward shedding by the limbs overhead.

DEPOSITS OF THE DIRECTED BLAST (PYROCLASTIC DENSITY FLOW) AND OF ATTENDANT AIR FALL (UNIT A)

STRATIGRAPHY

Gravel and sand layers (layers A1 and A2).—The stratigraphic unit at the base of the air-fall sequence, which beyond 20 km is a sandy silt only millimeters thick, thickens and coarsens to gravel and sand more than 1 m thick on the north flank of the volcano. Near the volcano a basal gravel (layer A1) decimeters

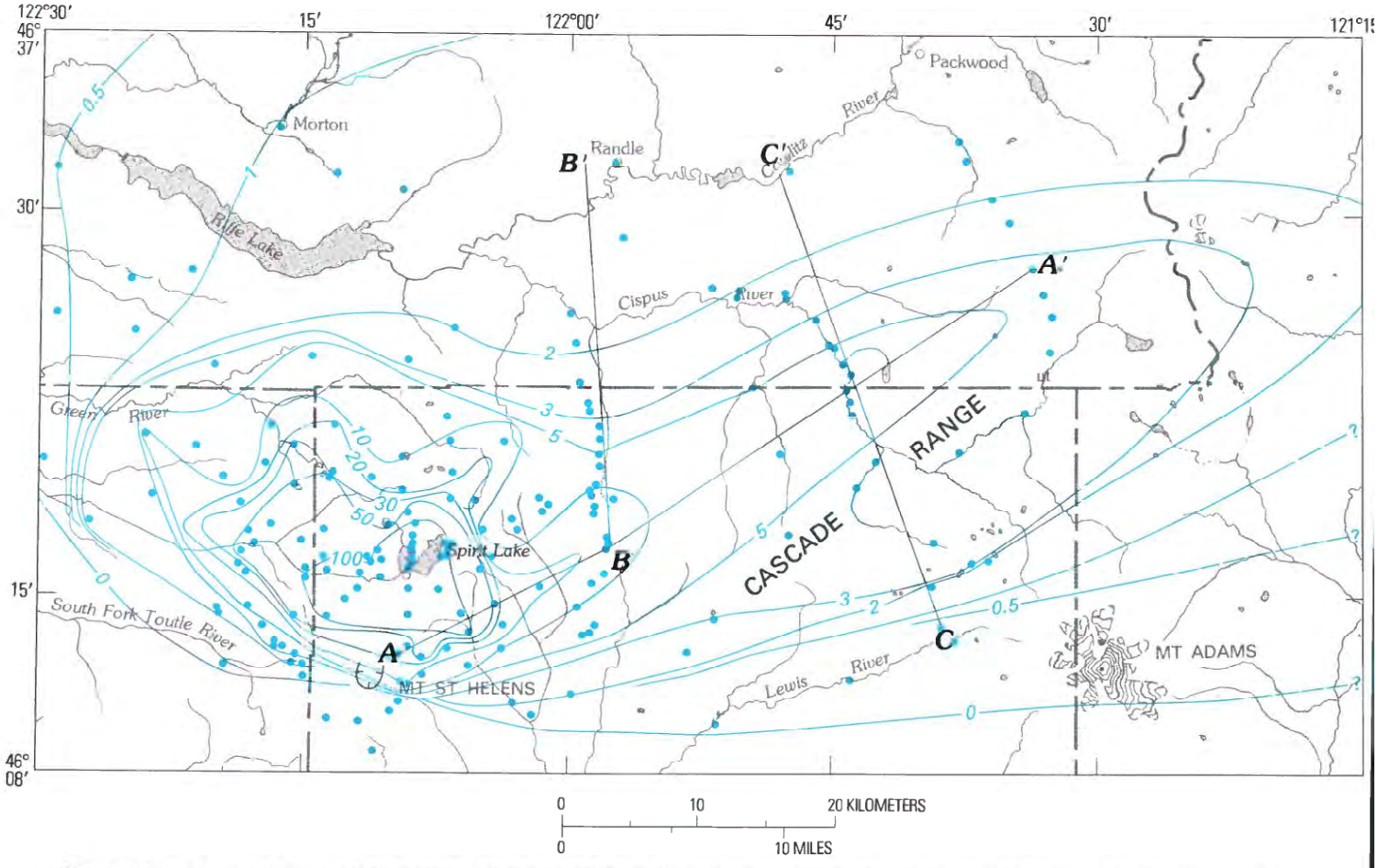

Figure 355.—Isopach map of total May 18 directed-blast (pyroclastic density flow) and air-fall deposits. Contour values in centimeters; thickness measured at sites indicated by blue dots.

thick is overlain by gray sand (layer A2) several centimeters thick.

Silt layer (layer A3).—Overlying layers A1 and A2 is a layer millimeters thick of moderately sorted dark-olive-gray[3] sandy silt (layer A3) characterized by pisolites (accretionary lapilli) (fig. 354*B*). Layer A3 is the only material of unit A distributed broadly beyond 20 km from the volcano. Within 15 km of the volcano on the north, the lower part of layer A3 does not contain pisolites, the upper part does; from 15 to 40 km north and out to 60 km east of the volcano, however, the basal part of layer A3 contains pisolites, whereas the upper part of the layer does not. The nonpisolitic phase of layer A3 composes the entire unit A beyond the outer limits of pisolites. At the base of this layer 20 km to the east, rare inconspicuous wisps of gray crystal-lithic ash probably accumulated during premagmatic eruptions from late March to mid-May (Sarna-Wojcicki, Waitt, and others, this volume). Layer A3 forms at least part of the basal unit of the distal air-fall sequence (Sarna-Wojcicki, Shipley, and others, this volume). Part of layer A3 fell wet and preferentially accumulated on limbs on the near side of coniferous trees. In the area of the directed blast (pyroclastic density flow) and broadly north to the Cowlitz valley and east to beyond Mount Adams, scorched branches, needles, and cones of conifers accumulated at the base of, within, or atop layer A3, although some are in the basal part of unit B.

[3]Colors measured moist from Munsell Soil Color Chart.

LATERAL VARIATIONS

Layers A1 and A2, which become thinner and finer grained away from the volcano, are restricted to the area of the downed and scorched timber (Waitt, this volume). The attendant layer A3 becomes gradually thinner away from the volcano, but rather abruptly pinches out on the volcano flanks (fig. 356).

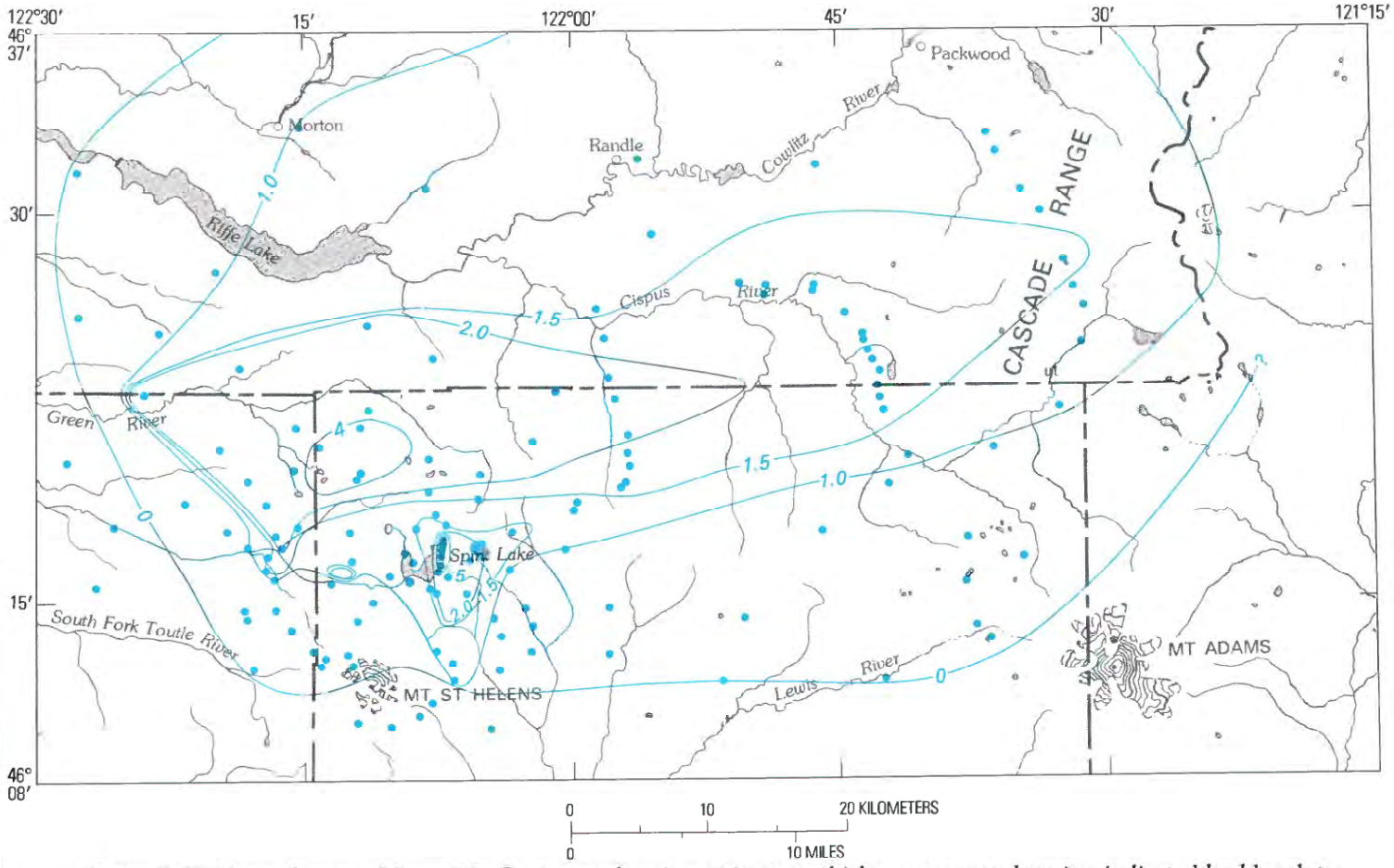

Figure 356.—Isopach map of layer A3. Contour values in centimeters; thickness measured at sites indicated by blue dots.

ORIGIN AND TIMING

Layers A1 and A2, confined to the area of devastation within 20 km of the crater on the west, north, and east, are the products of the directed blast (pyroclastic density flow) that began at 0833 PDT. Description and stratigraphy of layers A1 and A2 and discussion of the event appear in Waitt (this volume), Moore and Sisson (this volume), and Hoblitt and others (this volume).

Layer A3 extends some 50 km to the north and hundreds of kilometers to the east-northeast. Its basal stratigraphic position, content of juvenile dacite and scorched tree fragments, and other attributes (Waitt, this volume) relate this unit to the directed blast (density-flow). Unlike the materials of layers A1 and A2 that were directly deposited by the flow traveling close to the surface, the material of layer A3 drifted far downwind. The pisolites characterizing parts of this unit show that the silt rose high or fast enough to condense water. Eyewitnesses beyond the area of the ground-hugging blast (density-flow) cloud first experienced air fall as pisolites from a dark cloud that swept a few kilometers overhead. The downwind axis of thickness of layer A3 emanates from the area of maximum thickness of layer A3 that is 15 km north of the mountain— probably the area of dominant trajectory of A3 material ejected upward and northward from the mountain (Waitt, this volume).

The branches and cones deposited within layer A3 had been eroded by the blast on the flanks of Mount St. Helens. The tree fragments that fell on Mount Adams and other distal localities apparently were drawn up by the initial vertical column. The enormous updraft attending the rapid growth of the vertical column minutes after the beginning of the eruption developed a strong wind toward the volcano (Rosenbaum and Waitt, this volume). The cloud that had enveloped the flanks of the volcano was thus drawn up, and spread quickly to the north and east as a dark anvil-shaped cloud. Just after the base of this cloud passed over the Cowlitz valley, Mount Adams, and areas closer to the volcano, scorched tree fragments and pisolites began to fall (Rosenbaum and Waitt, this volume). The close stratigraphic association of scorched tree fragments with layer A3 far downwind independently corroborates the sequence assembled from the eyewitness reports. The material of layer A3 fell from about 0850 to 0930 PDT within 25 km of the mountain, and from about 0900 to 1000 PDT 30–70 km away (Rosenbaum and Waitt, this volume).

PUMICE-LITHIC AIR-FALL UNIT (UNIT B)

STRATIGRAPHY

At distances of 50–100 km along the axis of the air-fall plume and at closer distances along the margins of the plume, a single layer of pumice-lithic granule gravel to sand overlies unit A (fig. 354*A*). In proximal areas broadly distributed along the axis of the lobe, the unit thickens and coarsens toward the volcano and is divisible into two to four layers (figs. 354*B*, 357).

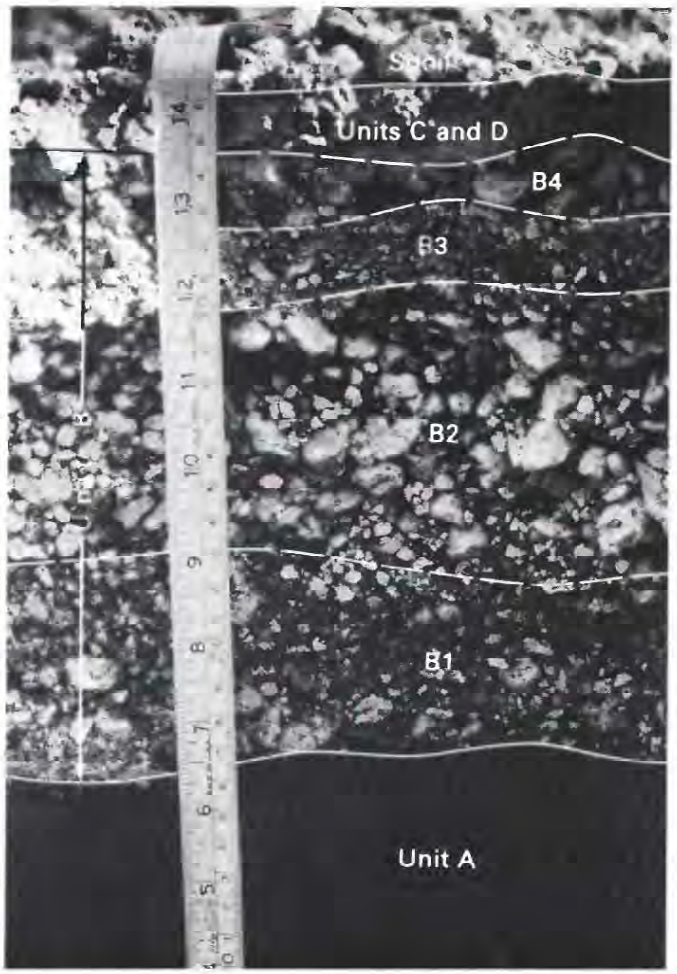

Figure 357.—Section view of units A, B, C, and D, showing divisions of unit B (layers B1, B2, B3, and B4). Right side of scale is graduated in centimeters; left side is in inches.

Basal lithic-rich layer (layer B1).—More than 50 percent by volume of the basal layer of unit B consists of lithic fragments and crystals; the remainder consists of pumice. The minor fraction of pumice in the layer extends to the base and is embedded in the top of layer A3. Near the volcano and along the axis of the lobe as far away as 25 km, layer B1 is lithic-pumice granule gravel; in more distal areas and along the margins of the lobe, it is a crystal-lithic-pumice sand. At some sites along the axis of the lobe 6–20 km from the vent, the base of layer B1 consists of scattered pumice pebbles or of a pumice-pebble zone 1–2 cm thick (fig. 357).

Lower pumice-rich layer (layer B2).—Layer B1 is overlain by a coarser layer B2 that contains 60–75 percent pumice by volume, the remainder being lithics and crystals. Near the volcano layer B2 is a pebble gravel that is generally reversely graded (fig. 357); along the margins at distances of from 20 to 50 km, it thins and fines to granule gravel, and in distal areas downwind fines to sand. This layer is about two phi-intervals coarser grained than the underlying layer B1: layer B1 consists of granule gravel where layer B2 is pebble gravel, or of medium sand where B2 is very coarse sand (fig. 357).

Upper lithic-rich layer (layer B3).—Along the axis of the lobe 10–25 km from the crater, layer B2 is overlain by a finer grained layer richer in lithic fragments and crystals, layer B3. This layer is recognized only at a few sites, and elsewhere it is obscured by the enclosing thicker and coarser layers B2 and B4.

Upper pumice-rich layer (layer B4).—Overlying layer B2 or layer B3 (where present) with a sharp contact is a coarse pale-brown layer containing 75 percent or more pumice by volume, the remainder lithic fragments and crystals (figs. 354*B* and 357). Unlike layers B1, B2, and B3, layer B4 has a conspicuous matrix of light-brown silt that also coats the pumice fragments. The mean and maximum sizes of pumice fragments in this layer are generally coarser than even those at the top of layer B2, although the layer is everywhere thinner than layer B2.

Toward the northern margin of the lobe of unit B near the volcano, layer B4 apparently thins to the point where it consists of scattered pumice granules and pebbles enclosed by unit C. Beyond 30 km from the volcano along this margin, layer B4 becomes sparser and finer grained, and the distinction between this layer and the light-brown unit C grows arbitrary. The merging of layer B4 with unit C, which in some places along the north margin of unit B both overlies and underlies pumice pebbles of unit B, indicates that layer B4 accumulated contemporaneously with part or all of unit C.

Sections near volcano with obscure stratigraphy.—On the east flank of the volcano, unit B does not show the internal stratification that exists only a few kilometers farther downwind but consists of a relatively thin, reversely graded layer of pumice and lithic fragments. Pumice blocks as large as 30 cm at the top of these sections protrude conspicuously through the overlying unit D. The generally finer lower part probably correlates with layer B1, and the coarser pumice at the top with layers B2 and B4, but contacts between these phases are obscure.

Large pumice fragments at and near the top of unit B on the east flank of the volcano have a pale-red interior that grades outward to a pale-orange rind 1.5 cm thick that in turn grades outward abruptly to a white rind 1.5 cm thick. The larger blocks thus apparently remained hot enough after they fell to oxidize.

LATERAL VARIATIONS

Within 5 km of the volcano, the air-fall section is notably thinner on the leeward (east) side of standing tree trunks than on the windward side, indicating an eastward component of fall. The 16-cm-thick section of units A, B, and D on the east flank of the volcano thickens to 20 cm against the windward side of a standing trunk but is only 3 cm thick against the leeward side. A lateral component to unit-B air fall is also shown by a 40-cm pumice block wedged from the west between two trunks.

The isopach map of unit B (fig. 358) shows that the axis of maximum thickness is alined with the central vent. The maximum thickness is some 15 km east-northeast of the crater, and the unit thins both downwind and toward the volcano. Isopleths of maximum pumice size, which splay broadly across the lobe of maximum thickness (fig. 358), illustrate the downwind and lateral decrease in particle size. The axis of coarseness is slightly clockwise of the axis of maximum thickness.

A stratigraphic cross section along the axis of the May 18 air-fall lobe illustrates downwind changes (fig. 359*A*). Unit B forms some 60–90 percent of the total thickness and therefore determines most of the

variation in total thickness. From its maximal thickness 15 km downwind, unit B is thinner and coarser grained upwind, and thinner and finer grained downwind. As unit B becomes finer grained downwind, the internal stratigraphy progressively disappears, so that beyond about 50 km only a single layer represents layers B1, B2, B3, and B4.

Stratigraphic cross sections across the main air-fall lobe (fig. 359*B* and 359*C*) illustrate lateral variations in the lobe. From its axis of maximal thickness at 25 km from the volcano to the margin of the lobe only 10 km north, unit B decreases in median grain size from granule gravel to sand, and its four internal layers merge into a single layer (fig. 359*B*).

ORIGIN AND TIMING

The alinement of the axes of coarseness and thickness with the central vent clearly identifies unit B as the deposit of the vertical column from the central vent. The column rose to 14 km or higher at least four times—twice in morning and twice in afternoon (Harris, Rose, and others, this volume; Rosenbaum and Waitt, this volume).

Layer B1.—The relatively low pumice content and fine grain size indicate a relatively low-energy eruptive column. Pumice occurs at the base of the unit, indicating that the initial vertical eruptive column, which within 30 min began depositing material downwind, carried juvenile pumice. The coarse pumice at the base of layer B1 in some places suggests a brief strong pulse at the beginning of the vertical eruption. Layer B1 probably formed from the initial to mid-morning eruption column.

Layer B2.—The coarser grain size and higher pumice content of layer B2 compared to layer B1 indicate that the vertical column itself became generally

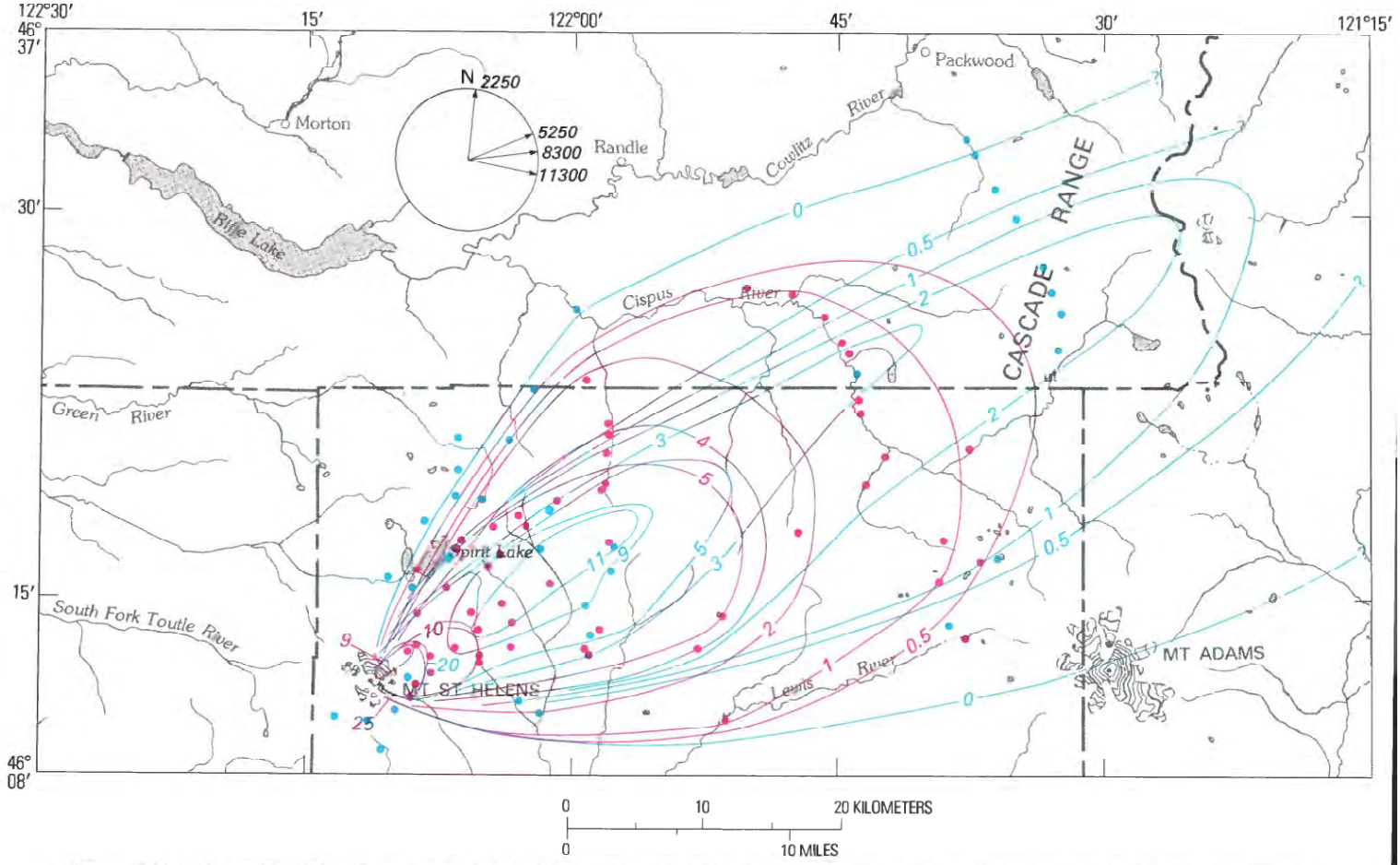

Figure 358.—Isopachs (blue lines and data points) and isopleths of maximum pumice size (red lines and data points) of unit B. Contour values in centimeters. Circular diagram shows approximate wind direction at various altitudes (in meters), from data supplied by U.S. National Meteorological Service.

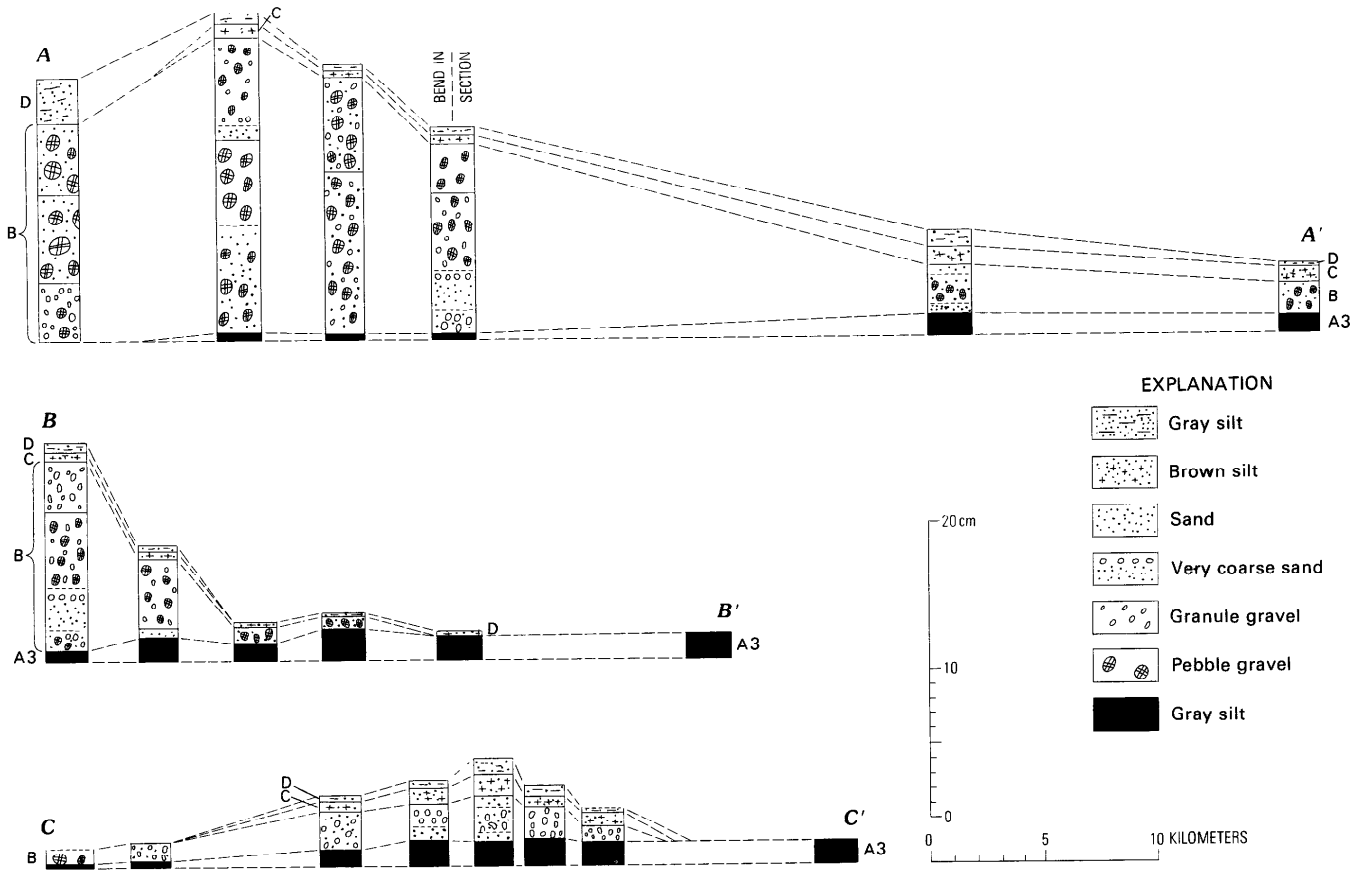

Figure 359.—Stratigraphic cross sections (see fig. 355 for locations). Section A-A', along axis of unit B lobe. Section B-B', across air-fall lobe about 25 km from volcano. Section C-C', across air-fall lobe about 40 km from volcano. Dashed lines indicate correlation of units A, B, C, and D.

more pumiceous, probably reflecting an increased rate of eruption of gas and pumice. The generally abrupt contact with layer B1 suggests that this change was abrupt. The general reverse grading of pumice fragments within layer B2 indicates that a trend toward higher altitude pumice ejection continued for some time. The lack of a pale-brown matrix suggests that this layer preceded the first ash flow. Layer B2 probably is the deposit of a relatively high column in late morning.

Layer B3.—The thin and sparsely recognized layer B3 records a fairly brief interval of a lower vertical column between the times of higher column represented by layers B2 and B4. The absence of a brown matrix indicates that this layer also preceded the first ash flow.

Layer B4.—The coarseness of layer B4 compared to layer B2 indicates a very gaseous pulse of the column; its relative thinness suggests that it accumulated during a shorter time interval than did layer B2 or from a less dense eruptive column. The abrupt appearance of the pale-brown silty matrix indicates an abrupt change in the vertical eruptive column. The matrix is similar in grain size and identical in color to the matrix of ash-flow deposits on the north flank of the mountain. Eruptions began to generate ash flows down the north flank at about 1217 PDT, (Rowley and others, this volume, table 42) when the eruptive column distinctly lightened in color (D. A. Swanson, oral commun., 1980). The abrupt appearance of a brown matrix in the air-fall deposit probably records this change. During magmatic eruptions in July and August, part of the pale-brown cloud convecting off north-flowing ash flows was drawn up into the vertical column simultaneously developing over the central vent (aerial-oblique photographs by R. P. Hoblitt, J. E. Vallance, and M. P. Doukas). The brown color of layer B4 probably resulted from a vertical eruptive column on May 18 that either similarly drew up part of the cloud convected off the ash flows,

or simply incorporated this fine material that was being generated by the ash-flow-producing explosions at the crater. Layer B4 thus originated from afternoon eruptions.

Variations in thickness and coarseness within unit B.—The maximum thickness of unit B some 15 km downwind from the volcano probably is due to the dominant trajectory of coarse particles. Ejected in the central column to a certain mean altitude, the coarse particles then drifted laterally in the prevailing windstream. Pumice fragments were produced in sizes ranging from 3-m blocks to micrometer-sized shards. The vertical column carried the fine fragments above the high-velocity windstream (above 13 km), from where they were transported laterally far downwind to form the white silt ash dominating the distal air-fall deposits (Sarna-Wojcicki, Shipley, and others, this volume). Few of the very coarsest fragments, on the other hand, even cleared the crater rim. The largest pumice block found on the lower east flank of the volcano is 40 cm in diameter. In the ash-flow deposits, however, 1-m pumice blocks are common and some are even larger. Such large fragments apparently remain low enough in the eruptive column that they can be transported from the crater area only by relatively dense ash flows. Of the coarse fragments thrust upward by the vertical column, a zone of maximum concentration develops at some altitude range. By the time this mode of coarse pumice and lithics has fallen to the ground, it has been translocated many kilometers downwind. Coarser fragments, not ejected as high and less influenced by the prevailing windstream than finer fragments, fall closer to the volcano. Having less volume, these coarser fragments produce a thinner layer.

The axis of maximum thickness is slightly counterclockwise of the axis of maximum coarseness (fig. 358). The low-level wind on May 18 was northward of the east-northeastward high-level wind that carried the plume. As material fell from the high-level plume, the lower level winds winnowed the finer material from the south to the north side of the plume. This pattern in unit B on May 18 resembles the pattern in more recent air-fall lobes, in each of which the axis of maximum thickness is displaced from the axis of maximum pumice size in the direction of the low-level winds (Waitt and others, this volume).

The May 18 unit B lobe, however, differs from the later air-fall lobes in that, in addition to coarse pumice at the southern margin of the lobe, some coarse pumice also lies sparsely along the northern margin. The main cause of this complication is that the isopleth map is of the entire unit B, which includes three relatively coarse layers that probably fell during three discrete episodes of high eruptive column between early morning and mid-afternoon of May 18. Between morning and late afternoon low-level winds had shifted northward. Many of the largest pumice fragments on the north half of the lobe are brownish and lie within unit C, and probably belong to layer B4, whereas coarse pumice near the southern margin is not brown and probably belongs to layer B2 or B1. The isopleth map thus mixes the results of sublobes influenced by gradually changing wind directions. The apparent northward displacement of the axis of thickness of layer B4 from the axis of layer B2 and the broad splay of the isopleth contours seem to reveal a gradual counterclockwise rotation of the axis of fallout during May 18—the abundant coarse pumice on the south having fallen from morning eruptions, the sparse coarse pumice on the north from afternoon eruptions.

PALE-BROWN SAND AND SILT (UNIT C)

STRATIGRAPHY

In the north-through-northeast sector a layer of pale-brown to light-brownish-gray silt to sand (unit C) overlies layer A3 and unit B. At a distance of 20 km along the axis of the air-fall lobe, the unit is a silty, medium to fine sand about 2 cm thick; it thins northward, southward, and downwind (to the east-northeast) to silt only a few millimeters or less in thickness. Where the material is fine sand or coarser, it probably contains the distal facies of layer B4. South and east of Spirit Lake rare pumice pebbles, probably of layer B4, are embedded near the top of unit C. Unit C thickens to several decimeters thick just north of the ash-flow deposits. Near Spirit Lake unit C comprises three layers—a coarser pumiceous layer divides a lower fine layer from an upper fine layer (figs. 354*B*, 360).

Lower silt (layer C1).—The lower layer (C1) is massive pale-brown silt to fine sand 0.5–2 cm thick. On the spur between the arms of Spirit Lake, this layer consists partly of pale-brown pisolites as much as 8 mm in diameter, but on the east side of the lake in Harmony Falls basin pisolites occur only in a rela-

tively thin zone near the base of the layer. Some of the pisolites have spherical cores of gray silt, which are pisolites reworked from the underlying layer A3. The basal contact with layer A3 is sharp, and at the spur between the arms of the lake it is channeled a few millimeters into layer A3. In places there are loading structures caused by layer C1 deforming the upper surface of layer A3 (fig. 360). The upper contact of layer C1 with layer C2 ranges from sharp to gradational.

Pumice sand (layer C2).—The middle layer of unit C, 0.2–0.5 cm thick near Spirit Lake, is of white pumice and lithic coarse to medium sand with a meager pale-brown silt matrix. Its upper contact with layer C3 is sharp. On the ridgecrest just southeast of Spirit Lake, where there are only two layers of unit C, layer C2 forms the basal coarse sand that is overlain by massive silt (layer C3).

Upper silt (layer C3).—The upper layer of unit C is massive pale-brown silt 2–3 cm thick that is similar to layer C1 but does not contain pisolites.

LATERAL VARIATIONS

Unit C is confined to the north half of the total air-fall lobe. The isopach map clearly shows that unit C thickens not toward the central crater, but toward the lower slope of the volcano about 8 km north of the crater (fig. 361). This is not only the area of ash-flow emplacement, but is also where one or more explosive secondary phreatic vents were active in late afternoon of May 18.

Unit C appears complex in figure 359*A* partly because the line of section is across the south half of the lobe of unit C, is oblique to the axis of unit C, and close to the volcano misses the lobe altogether. Unit C generally thins and fines to the east-northeast, and becomes stratigraphically less complicated. The stratigraphic relation of unit C to layer B4 in the northern part of the air-fall lobe becomes ambiguous beyond 20 km from the volcano. The pale-brown silt and sand beyond 30 km from the volcano probably is both unit C and layer B4, which seem to have resulted from different but contemporaneous events.

ORIGIN AND TIMING

Unit C, which thickens westward toward the ash-flow deposits just west of Spirit Lake some 8 km north of the crater, clearly originated from the north-side ash flows. On Coldwater Ridge, just north of the ash-flow plain, unit C is absent on steep slopes but thickens to many decimeters in adjacent flat areas or depressions. The ash deposited there originated by elutriation from the ash flows and was carried beyond the flows as turbulent clouds (Rowley and others, this

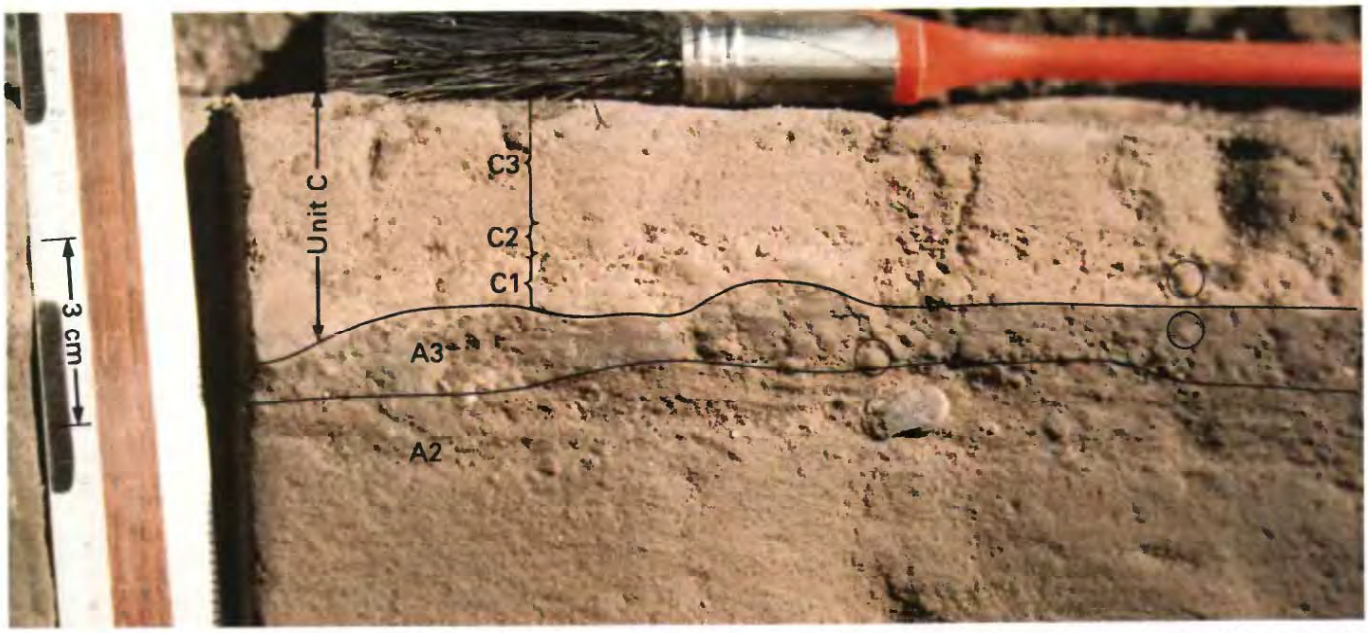

Figure 360.—Photograph taken near Spirit Lake showing layers of unit C and disconformable contact with layer A3. Pisolites, some of which are circled, can be seen in layers A3 and C1.

volume). Being fine grained, hot and dry, the ash deposited on steep slopes by the turbulent ash clouds subsequently flowed downslope to more level sites. These thick deposits gradually thin to only a few centimeters many kilometers to the north and east (fig. 361), where their relatively uniform thickness indicates air-fall deposition.

The sequence of three layers near Spirit Lake records a sequence of events related to the ash flows. The basal layer C1 lies disconformably on layer A3. Some of the 2- to 4-mm gray pisolites eroded from layer A3 were rolled into larger pisolites concentrically layered with pale-brown silt. Most of the large pisolites, however, are entirely of the pale-brown silt indigenous to unit C. The pisolitic layer is thickest, and the relief on its contact with layer A3 greatest, from 10 to 100 m above the new lake surface on the spur between the arms of the lake (figs. 353, 360); sparser pisolites occur at the northeastern margin of the lake. The pisolites indicate that water condensed on the ash particles, causing them to adhere to one another. These characteristics suggest that layer C1 originated as the distal edge of the largest ash flows that swept into the southern margin of the lake. The turbulent clouds rolling beyond the ash flows, being less dense than water, continued across the lake. Acquiring moisture from the lake surface, the ash particles formed pisolites that were swept along by the laterally moving cloud and upslope on the far side of the lake. Layer C1 is absent on the ridge crest just southeast of Spirit Lake because the momentum of the turbulent, denser-than-air ash cloud carried the

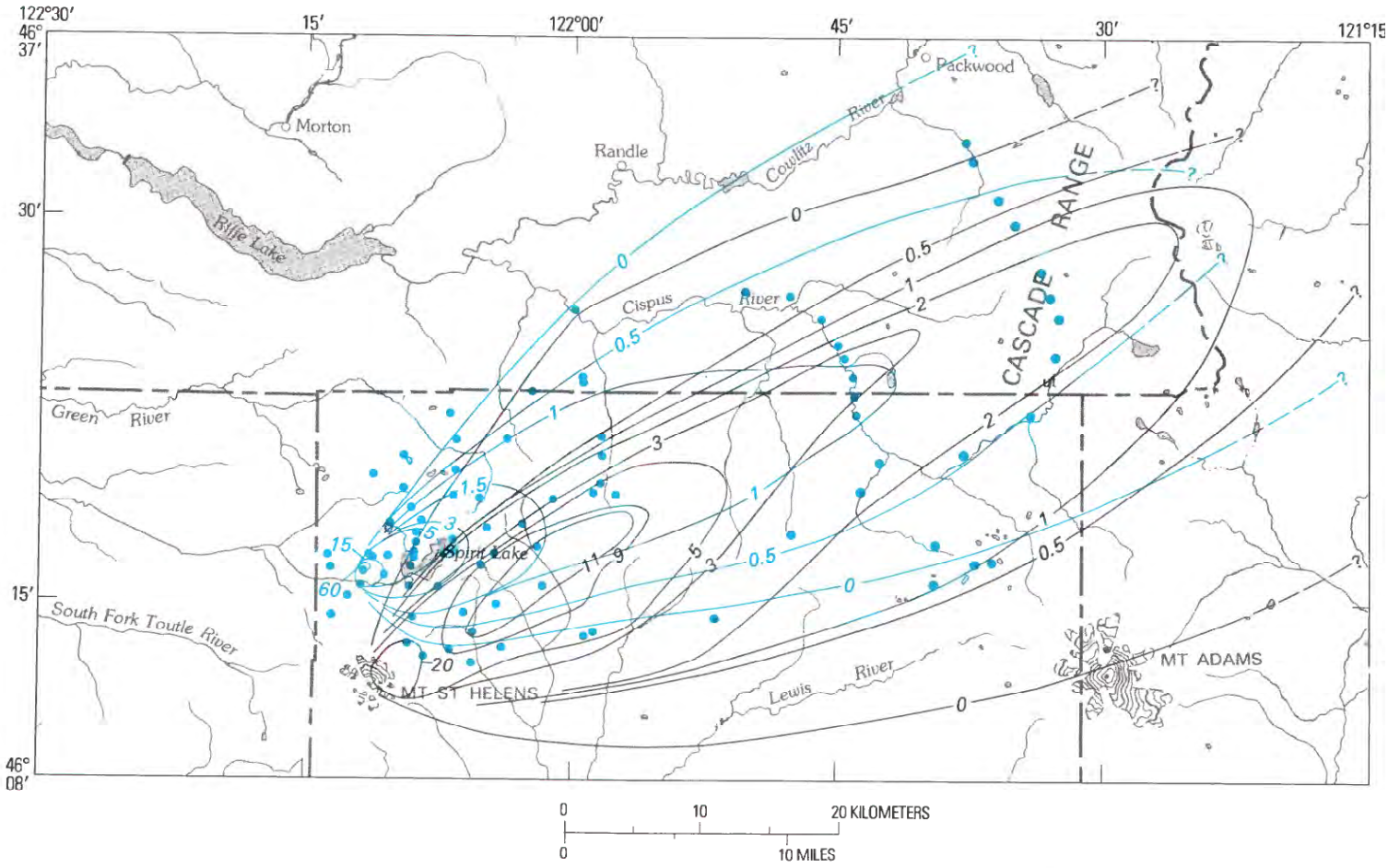

Figure 361.—Isopach map of units B (screened gray) and C (blue contours and data points). Contour values in centimeters. Thickness of unit C measured at sites indicated by blue dots; see figure 358 for data points where thickness of unit B was measured.

cloud northward at low levels. The bulk of layer C1, however, probably is air-fall material of a cloud that merely convected off the ash flows.

Layer C2 represents an event energetic enough to propel coarse sand- to gravel-sized pumice high enough into the windstream to be partly winnowed of the pale-brown silt. This layer may record the initiation of the secondary phreatic column that reworked ash-flow material from late afternoon until at least 2045 PDT. The principal secondary column was only 1 km upwind from the west margin of Spirit Lake.

Layer C3, which lacks pisolites, seems to be mainly fallout from the cloud convected off the ash flows; it probably also is air-fall silt from the plume of the secondary phreatic columns as they became smaller. This unit overlies layer C2, attributed to the most energetic phase of the phreatic columns. Layer C3 therefore must date from late afternoon and evening.

During most of the afternoon of May 18, the cloud convecting up from the north-side ash flows rose 2 km or more; the plume of the phreatic eruption that reworked newly accumulated ash-flow material rose to altitude 3 km in late afternoon and evening. Beyond 15 km east-northeast of the ash-flow plain, the single unit of silt to fine sand of unit C probably is material that drifted downwind from three sources: turbulent clouds propelled laterally off the ash flows, clouds convecting upward from them, and plumes from phreatic eruptions reworking the hot ash-flow deposits.

UPPER GRAY SILT (UNIT D)

DESCRIPTION

Northeast and east-northeast of the volcano, the May 18 air-fall deposits are capped by a layer of gray silt a few centimeters thick close to the volcano but only millimeters thick beyond 20 km (figs. 354, 357). Unit D is texturally similar to the pale-brown silt of unit C, but when wet is sharply distinguished from unit C by its gray color. Unlike layer A3, unit D is well sorted and does not contain tree fragments.

LATERAL VARIATIONS

On the lower east flank of the volcano, the windward sides of trees are notably plastered with gray silt. As unit A is nearly absent here, this silt must be from unit D, showing that even the latest air fall on May 18 fell with a lateral component of movement. Unit D decreases only slightly in grain size downwind.

Unit D is thickest on the flank of the volcano but also has an amplified thickness some 40 km from the vent (fig. 362). This amplified thickness probably was caused by the common trajectory of the most abundant particles in the eruptive column. The maximum-thickness axis of unit D is displaced slightly northward from the maximum-thickness axis of unit B.

ORIGIN AND TIMING

The axis of maximum thickness of unit D is alined with the central crater, and the unit overlies both units B and C and interfingers with neither. Unit D therefore must have accumulated from the plume from the vertical column after 1900 PDT, when the top of the column had declined to below altitude 5.5 km but continued to be dark with emitted ash. The amplified thickness 40 km from the mountain is similar to the amplified thickness in fine air-fall deposits of May 18, May 25, and June 12, amplified thicknesses that formed 40–250 km downwind of central eruptive columns ejected to altitudes of from 12 to 18 km (figs. 336, 344, and 345). The amplified thickness of unit D probably resulted from the downwind trajectory of fine particles that had been ejected roughly to altitude 4–5 km during the waning phase of the May 18 eruption. Low-level winds were counterclockwise of the high-level winds throughout May 18. The material of unit D, ejected to comparatively low altitude, was moved from the vent by a windstream that was northward of the high-altitude windstream that carried most of the material of unit B.

SURFICIAL PUMICE (UNIT E)

DESCRIPTION

In the coniferous forest beyond the devastated area but broadly along the axis of unit B, scattered pumice pebbles overlie unit D (fig. 363). This layer is present only beneath the branches of living trees. It is absent in the area of downed timber, in natural clearings within the forest, and along roads and other man-made clearings.

ORIGIN AND TIMING

For many days after May 18, coarse pumice fell from the branches of living conifers, where it had been selectively trapped on May 18. Because of their delayed arrival at the ground surface, these pumice fragments were deposited not with unit B where they stratigraphically belong, but upon the surface of unit D, which had become coherent because of rain. The pumice overlying unit D 40 km east of the volcano has a median size of about 7 mm, whereas that of the primary air fall (unit B) is only 1.5 mm. Yet clearly the two layers were part of a single population delivered simultaneously to the area of their separate accumulation.

This delayed pumice fall was followed by air-fall pumice on July 22, whose distribution corresponded closely to that of the May 18 air-fall lobe (Waitt and others, this volume). The scattered pumice of May 18 unit E and of July 22 mingled to constitute the single discontinuous layer that overlies unit D.

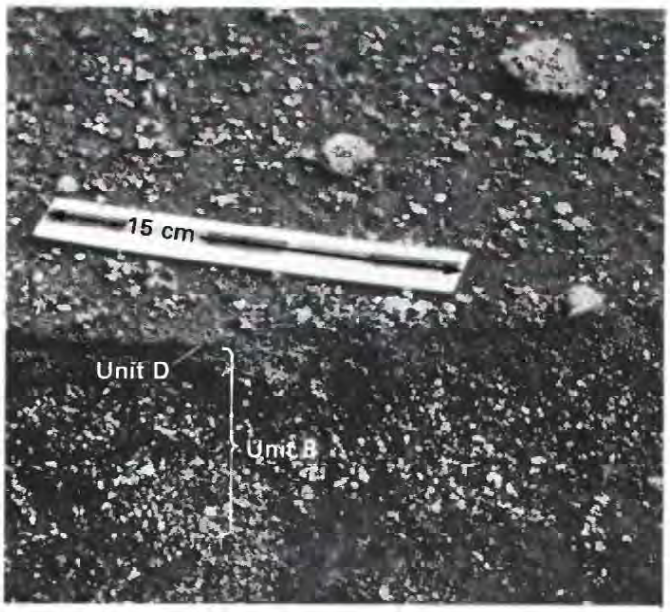

Figure 363.—Scattered pumice of unit E, found only in coniferous forest, overlying unit D.

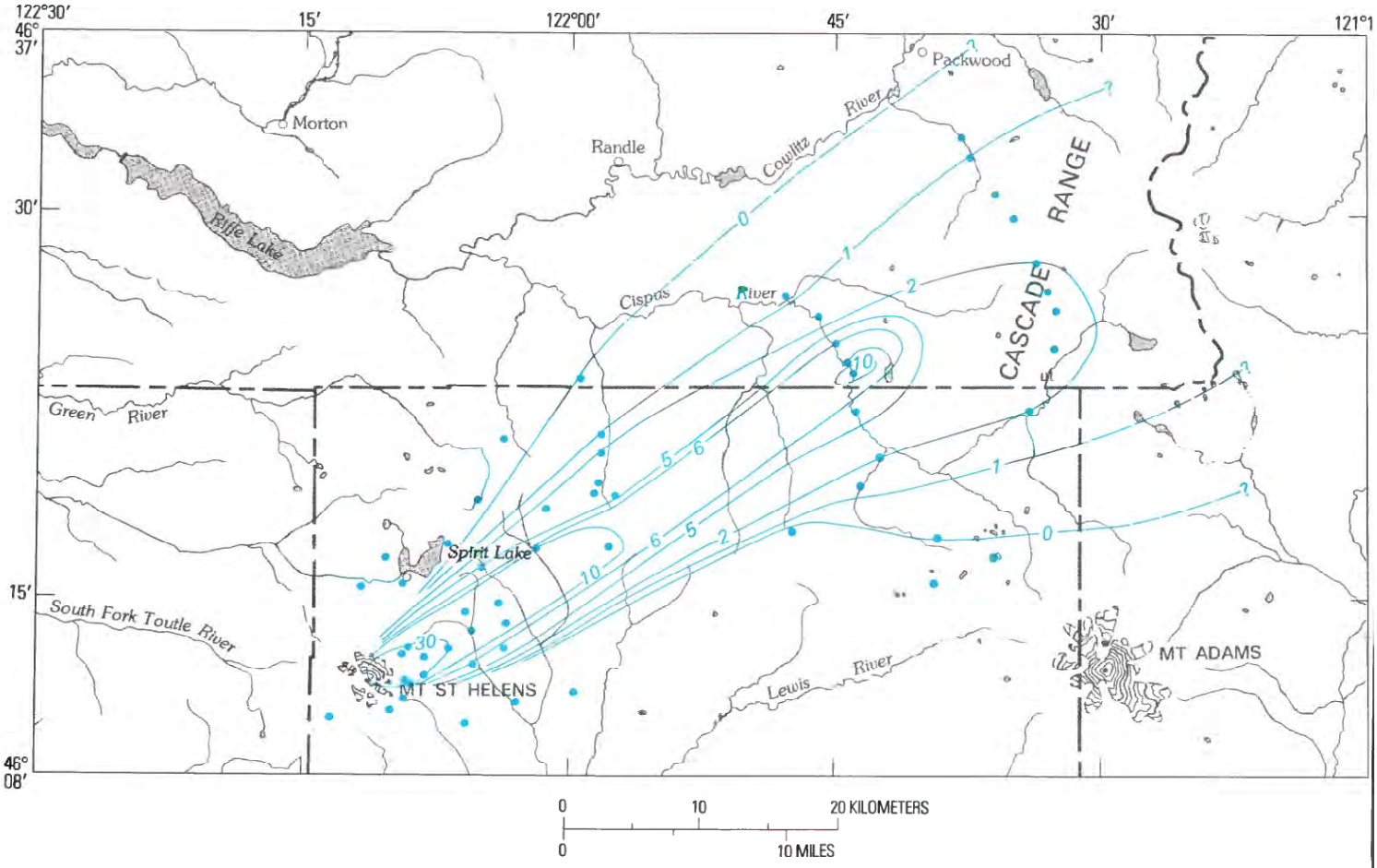

Figure 362.—Isopach map of unit D. Contour values in millimeters. Thickness measured at sites indicated by blue dots.

INTERPRETATION OF STRATIGRAPHY OF ANCIENT AIR-FALL DEPOSITS

Because the units and layers of the May 18 deposits can be traced to thicker deposits that are easily exposed by shallow excavation, and because many of these units and layers can be logically attributed to events that were observed on May 18, the origin of these deposits is relatively clear. The sequence of 10 distinguishable air-fall layers all deposited as a consequence of the May 18 eruption is an example to aid interpretation of stratigraphic sections of ancient tephra. Viewed from the future, the sharp boundaries in texture or color between units A, B, C, and D, or between layers A2 and A3 or layers C2 and C3, could be taken as evidence of separate events spanning considerable time. Yet these units are all products of a single day's activity at Mount St. Helens. The layer of fir needles in some areas concentrated atop layer A3 also could be taken to imply a time break during which nearby standing trees casually shed debris onto the new surface; whereas they are needles eroded from trees only an hour or so earlier. A future ^{14}C date obtained for this layer will not only be a maximum-limiting age for the overlying layer and a minimum-limiting age for the underlying layer, but will also closely date both layers.

RELATIVE MAGNITUDE OF ERUPTION

Whereas the thickest proximal accumulation of May 18 unit B is about 25 cm, on the north-through-northeast sector, ancient air-fall pumice accumulations—layers Yn (3400 B.P.), Wn (450 B.P.), and T (A.D. 1800) (Crandell and Mullineaux, 1978, figs. 2, 9)—are as thick as 1 m. In proximal areas the coarse air-fall material of May 18 was thus quite thin compared to three major air-fall lobes from the volcano. East of the Cascade Range, however, the fine air-fall deposit of May 18 forms a continuous layer almost a half-centimeter thick along the axis of the lobe. In unplowed areas this layer probably will remain as a permanent white-ash layer comparably thick to some of the ancient Mount St. Helens ash lobes in eastern Washington (Waitt, 1980, fig. 11*A*).

In the proximal area the thickness of each air-fall unit decreases exponentially downwind from the vent (fig. 364). The magnitude of the May 18 eruption relative to other eruptions of Mount St. Helens and other Cascade Range volcanoes can be compared by plotting thickness of air-fall lobes as a function of distance from the vent. The unit B lobe is generally one-half to one-fourth as thick as pumice layer T, the thickest air-fall deposit of the early 19th-century eruptive episode. The unit B lobe is 4 or 5 times thicker than the 1842–43 lobe, the largest air fall during the mid-19th-century episode (Harris, 1976, p. 178–181). The 1842–43 lobe is similar in thickness to unit D, the final low-energy central-column deposit of May 18.

Beyond 10 km from the volcano, the thickness of the entire May 18 lobe—units A, B, C, and D together—is similar to the thickness of ancient pumice layer T (fig. 364), which is also similar to other lobes

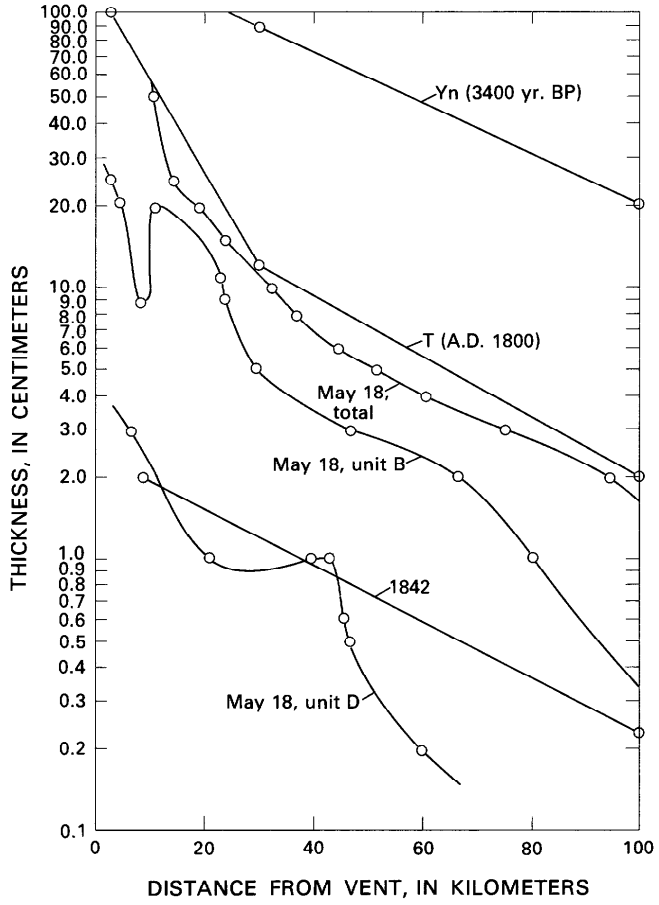

Figure 364.—Plot of thickness of air-fall lobes from Mount St. Helens as a function of distance downwind of volcano. Data from pre-1980 eruptions from Crandell and Mullineaux (1978, figs. 2, 9). Open circles, data points.

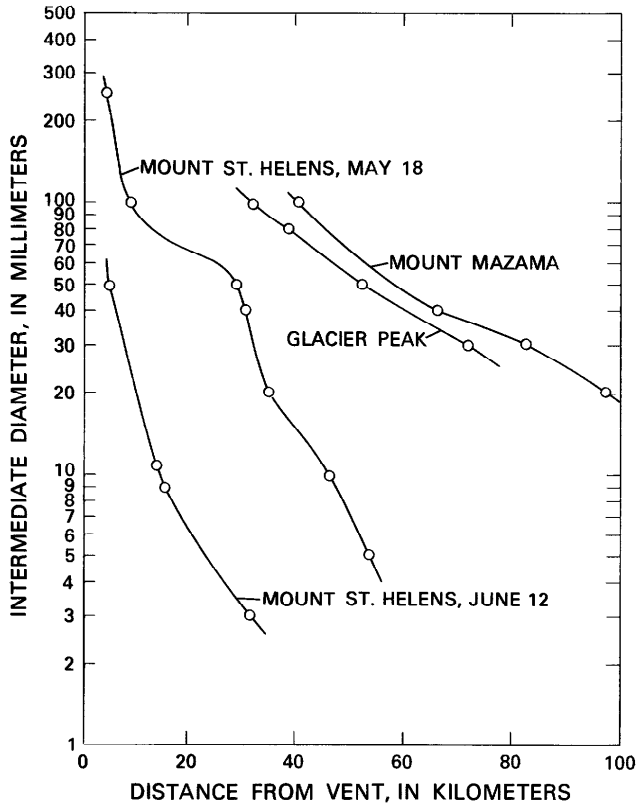

Figure 365.—Plot of intermediate diameter of largest pumice fragments as a function of distance downwind from volcano. Data from Glacier Peak and Mount Mazama from Porter (1978, fig. 8). Open circles, data points.

during each of two earlier highly explosive episodes—layers We and Ye (Crandell and Mullineaux, 1978). Except near the volcano, these lobes and the total May 18, 1980, lobe were each roughly 5 times thinner than Mount St. Helens lobe Wn (450 yr B.P.), and 10 times thinner than lobe Yn (3400 yr B.P.) and than the two thickest lobes from the eruptions of Glacier Peak 11,250–13,000 yr B.P. (fig. 364).

Maximum particle size in air-fall deposits, a measure of the transportational competence of the eruptive column and the prevailing windstream, also decreases exponentially with distance downwind from the vent (fig. 365). Maximum pumice size of the Mount St. Helens May 18 unit B is 5–10 times larger than that of post-May 18 eruptions from Mount St. Helens (fig. 376). But maximum pumice size of unit B is 5–10 times smaller than that from large ancient eruptions of the Cascade volcanoes Glacier Peak and Mount Mazama (fig. 365).

REFERENCES CITED

Crandell, D. R., and Mullineaux, D. R, 1978, Potential hazards from future eruptions of Mount St. Helens volcano, Washington: U.S. Geological Survey Bulletin 1383-C, 26 p.

Folk, R. L., 1974, Petrography of sedimentary rocks: Austin, Texas, Hemphill Publishing Co., 182 p.

Harris, S. L., 1976, Fire and ice—The Cascade volcanoes: Seattle, The Mountaineers, 316 p.

Hoblitt, R. P., Crandell, D. R., and Mullineaux, D. R., 1980, Mount St. Helens eruptive behavior during the past 1,500 years: Geology, v. 8, no. 11, p. 555–559.

Mullineaux, D. R., Hyde, J. H., and Rubin, Meyer, 1975, Widespread late glacial and postglacial tephra deposits from Mount St. Helens volcano, Washington: U.S. Geological Survey, Journal of Research, v. 3, p. 329–335.

Porter, S. C., 1978, Glacier Peak tephra in the North Cascade Range, Washington: stratigraphy, distribution, and relationship to late-glacial events: Quaternary Research, v. 10, p. 30–41.

Waitt, R. B., Jr., 1980, About forty late-glacial Lake Missoula Jokulhlaups through southern Washington: Journal of Geology, v. 88, p 653–679.

Wentworth, C. K., 1922, A scale of grade and class terms for clastic sediments: Journal of Geology, v. 30, p. 377–392.